

Review

Dual-targeted nanomedicines for enhanced tumor treatment

Yaqin Zhu^{a,b}, Jan Feijen^{a,b,*}, Zhiyuan Zhong^{a,**}^a Biomedical Polymers Laboratory, and Jiangsu Key Laboratory of Advanced Functional Polymer Design and Application, College of Chemistry, Chemical Engineering and Materials Science, Soochow University, Suzhou, 215123, PR China^b Department of Polymer Chemistry and Biomaterials, Faculty of Science and Technology, MIRA Institute for Biomedical Technology and Technical Medicine, University of Twente, P.O. Box 217, 7500 AE, Enschede, The Netherlands

ARTICLE INFO

Article history:

Received 5 September 2017

Received in revised form 9 November 2017

Accepted 23 December 2017

Available online 8 January 2018

Keywords:

Nanomedicine

Dual-ligand

Tumor-targeted delivery

Tumor therapy

Receptor-mediated endocytosis

Cell-penetrating peptides

Targeting efficacy

ABSTRACT

Based on the overexpression of specific receptors on tumor cells, active targeting nanomedicines have been developed with the ability to efficiently deliver imaging agents in the tumor area or anticancer drugs into tumor cells via receptor-mediated endocytosis. Nevertheless, the efficacy of single-ligand nanomedicines is still limited due to the complexity of the tumor microenvironment. In recent years, dual-ligand nanomedicines have attracted a lot of interest, because these nanomedicines endowed with versatile functions, have the potential to improve the efficacy of tumor-targeted delivery. In this review, an overview of various dual-ligand nanomedicines for tumor targeted therapy will be presented, the role of cell penetrating peptides in combination with targeting ligands will be discussed and factors that affect the targeting efficacy of dual-ligand nanomedicines will be evaluated.

© 2017 Elsevier Ltd. All rights reserved.

Contents

Introduction.....	66
Dual molecular targeting	66
Dual targeting with RGD	66
Dual targeting with HA	70
Dual targeting with transferrin	72
Other dual molecular targeting	74
Targeting ligand combined with cell penetrating peptides.....	76
Dual-targeting with one ligand.....	81

Abbreviations: ADCs, antibody drug conjugates; ApoE, apolipoprotein E; BBB, blood-brain barrier; BCECs, brain capillary endothelial cells; BCSCs, breast cancer stem cells; BSA, bovine serum albumin; CD44, cluster determinant 44; CPPs, cell-penetrating peptides; CYC, cyclopamine; DBCO, dibenzocyclooctyl; DOX, doxorubicin; DSPE, distearoyl phosphoethanolamine; DTX, docetaxel; ECM, extracellular matrix; EGF, epidermal growth factor; EGFR, epidermal growth factor receptor; EMA, European Medicines Agencies; EPR, enhanced permeability and retention; ER, estrogen receptor; FA, folic acid; FDA, US Food and Drug Administration; FR, folic acid receptor; GTC, galactose-modified trimethyl chitosan-cysteine; HA, hyaluronic acid; HSPGs, heparin sulfate proteoglycans; HER2, human epidermal growth factor receptor-2; HUVEC, human umbilical vein endothelial cell; IFP, interstitial fluid pressure; L-Cys, L-cysteine; LDL, low density lipoprotein; Lf, lactoferrin; LfR, lactoferrin receptor; LRP, low-density lipoprotein receptor-related protein; MAL, maleimide; MDR, multidrug resistance; MMP-2, matrix metalloprotease 2; MRI, magnetic resonance imaging; MSNs, mesoporous silica nanoparticles; NGR, Asn-Gly-Arg; Sulfo-NHS, N-hydroxysulfosuccinimidate; NRP1, neuropilin-1; PAMAM, poly (amidoamine); PCL, poly(ϵ -caprolactone); PE, phosphatidylethanolamine; PEG, polyethylene glycol; PEI, polyethyleneimine; P-gp, P-glycoprotein; PLGA, poly (lactic-co-glycolic acid); PPE, polyphosphoester; PTX, paclitaxel; QD, quantum dots; RES, reticuloendothelial system; RGD, Arg-Gly-Asp; SDS-PAGE, sodium dodecyl sulfate polyacrylamide gel electrophoresis; SLNs, solid lipid nanoparticles; SP, substance P; STR-RX, stearylated oligoarginine; tefrac, tetraiodothyroacetic acid; Tf, transferrin; Tfr, transferrin receptor; TGN, TGNYKALPHNG; TPP, triphenylphosphonium; VEGF, vascular endothelial growth factor; VEGFR, vascular endothelial growth factor receptor.

* Corresponding author at: Biomedical Polymers Laboratory, and Jiangsu Key Laboratory of Advanced Functional Polymer Design and Application, College of Chemistry, Chemical Engineering and Materials Science, Soochow University, Suzhou, 215123, PR China.

** Corresponding author.

E-mail addresses: j.feijen@utwente.nl (J. Feijen), zyzhong@suda.edu.cn (Z. Zhong).

Conclusions	82
Acknowledgement	83
References	83

Introduction

The last few decades have witnessed significant progress in the development of nanomedicines, showing great promise in cancer therapy. Anticancer compounds including drugs, genes and proteins, regardless hydrophobic or hydrophilic, can be well conjugated to or incorporated in nanocarriers. When applied *in vivo*, nanocarriers can enhance the stability of anticancer compounds by protecting them from biodegradation or excretion, reducing their toxicity and enhancing the maximum tolerated dose (MTD) by changing their systemic distribution, thereby improving the efficacy of anticancer compounds [1,2]. So far, various kinds of nanomedicines such as antibody drug conjugates (ADCs), drug conjugates and nanocarriers for cancer therapy have been approved by the US Food and Drug Administration (FDA) and European Medicines Agencies (EMA) [2]. In the past years, the major underlying mechanism proposed for nanomedicine based cancer therapy was passive targeting associated with the enhanced permeability and retention (EPR) effect [3]. However, more and more studies have revealed that the EPR effect, although present in animals like mice, plays a less important role in humans due to tumor heterogeneity or lack of fenestrations in the tumor endothelium [4,5]. Active-targeting based on ligand-receptor recognition may show better efficacy than passive targeting in human cancer therapy and several active-targeting nanomedicines have already progressed into clinical trials [6–8]. For example, ANG1005, a novel peptide-paclitaxel conjugate, shows blood-brain barrier (BBB) penetrating ability and antitumor activity in metastatic breast cancer (BC) patients with recurrent brain metastasis (BM) *via* low-density lipoprotein receptor-related protein (LRP-1)-mediated transcytosis and endocytosis, as demonstrated by a phase II clinical study [9]. Since active targeting is based on the recognition and binding of ligands to tumor cell surface receptors, the targeting effect is, of course, affected by the receptor expression. However, It is well known that the receptors (surface markers) of tumor cells change dynamically with tumor progression [10,11]. In addition, ligand-receptor binding is a saturable process as the recycling and synthesis of receptors takes time [12]. It was also reported that different receptors are often upregulated on tumor cells and drug resistance is often associated with upregulation of alternative receptors as well as pathway switching between two receptors [13,14]. These factors will affect the delivery efficiency of single-ligand nanomedicines, thereby reducing drug efficacy. Compared with single ligand targeting that may result in uncontrollable and fluctuating targeting efficiency, dual-ligand strategies may lead to better cell selectivity and cellular uptake in cancer therapy. Pre-clinical studies and clinical trials demonstrated that dual-targeted therapy for several HER2 positive cancers with a combination of trastuzumab antibody (anti-HER2) and lapatinib (EGFR/HER2 tyrosine kinase inhibitor) resulted in better antitumor efficacy than monotherapy [15–17]. The advantages of using dual-targeting antibodies have been introduced in detail by Kontermann [18]. In this review we will focus on the design and application of nanosystems with dual ligands for tumor-targeted therapy (Table 1). Based on different combinations of ligands, different effects can be achieved. Firstly, combining two targeting ligands may improve the selectivity and uptake of the nanomedicine by specific tumor cells, provide the possibility to target different cells, which are involved in the development of the tumor, or achieve both cellular and organelle-

Scheme 1. Three different types of dual-molecular targeting. (A) Dual-targeting nanocarriers target one kind of cell (a) that overexpresses receptors for ligand X or Y recognition. (B) Dual-targeting nanocarriers simultaneously target cells (a) that overexpress one kind of receptor for ligand X recognition and cells (b) that overexpress another kind of receptor for ligand Y recognition. (C) Dual-targeting nanocarriers target cells that overexpress one kind of receptor on the cell membrane for ligand X recognition and another kind of receptor inside cells on nuclei or mitochondria for ligand Y or Z recognition.

specific targeting to realize precise delivery of anticancer agents to their intracellular therapeutic active site, therefore improving their antitumor efficacy. The second approach is combining targeting ligands with cell penetrating peptides (CPPs) to further enhance the cellular uptake of nanomedicine to specific tumor cells. In addition, dual-targeting using one ligand will also be discussed. Other approaches that aim at the combined use of nanosystems with one ligand and an external force (magnetic field) to concentrate the nanosystem in the tumor area [19–24] will not be further discussed in this review.

Dual molecular targeting

Dual molecular targeting is a strategy in which two ligands are used to target different receptors which may be either expressed on/in one type of cell or on different cells. The ligands used can be either combined in one molecule, or separately placed on the surface of the nanocarriers. Among these dual-ligand combinations, the most common ones are those in which a second ligand is combined with either RGD, HA or transferrin, since the latter ligands are overexpressed on various cancer cells and have been extensively studied. The combinations of ligands used can be generally classified into three different types based on the types of targeted cells and the action sites (Scheme 1). In the first type (Scheme 1A) two ligands target one kind of cell, which simultaneously overexpresses two kinds of receptors. The second type of dual-ligand targeting is that two ligands respectively target two kinds of cells (Scheme 1B). The third type of dual-targeting combines cell membrane targeting with intracellular organelle targeting (nuclear targeting or mitochondrial targeting) (Scheme 1C).

Dual targeting with RGD

Integrins, consisting of an alpha and beta chain, are a family of transmembrane glycoproteins and play an important role in cell signal transduction, gene expression, cell proliferation, apoptosis, invasion, metastasis, angiogenesis, and tumor progression [96]. The $\alpha_v\beta_3$ integrin is upregulated in both angiogenic endothelial cells and tumor cells. Cyclic or linear derivatives of RGD (Arg-Gly-Asp) oligopeptides, which have high affinity for $\alpha_v\beta_3$ integrin, have been widely studied in tumor-targeted delivery [97–100]. Therefore, combinations of RGD peptides with other ligands for dual molecular targeting have been frequently investigated. Kluza

Table 1
Examples of nanocarriers using dual-ligand strategies.

Dual-ligand strategies	Targets	Carrier	Cancer Model	Ref.
Dual molecular targeting <i>dual targeting with RGD</i>				
RGD/Anginex	$\alpha_v\beta_3$ integrin /galectin-1	liposomes liposomes	HUVEC cells B16F10 melanoma (in vivo MRI imaging)	[25] [26]
RGD/B6 cRGD/Tf	$\alpha_v\beta_3$ integrin/TfR $\alpha_v\beta_3$ integrin/TfR	polyplexes hyperbranched amphiphilic nanoparticles	DU145 and PC-3 cells HUVECs and HeLa cells	[27] [28]
RGD/Interleukin-13 RGD/Interleukin-13 RGD/substance P (SP)	$\alpha_v\beta_3$ integrin/ IL13R α 2 $\alpha_v\beta_3$ integrin/ IL13R α 2 $\alpha_v\beta_3$ integrin /neurokinin-1	PEG-PCL nanoparticles PEG-PCL nanoparticles liposomal nanoparticles	HUVECs and C6 cells (in vivo) C6 glioma cells (in vivo) U87MG and M21 cells (SPECT/CT imaging)	[29] [30] [31]
RGDS _D (KLA K LAK) ₂ RGD/estrone cRGD/AS1411 <i>dual targeting with HA</i>	$\alpha_v\beta_3$ integrin /mitochondria $\alpha_v\beta_3$ integrin/estrogen receptor $\alpha_v\beta_3$ integrin /nucleolin	chimeric peptide hydrogel gold nanoclusters	U87MG cells MCF-7 cells (in vivo) U87MG cells (in vivo)	[32] [33] [34]
HA/FA HA/FA HA/FA HA/tetrac HA/GE11	CD44/FR CD44/FR CD44/FR CD44/ $\alpha_v\beta_3$ integrin CD44/EGFR	micelles micelles liposomes solid lipid nanoparticles nanogels	MCF-7 cells MCF-7 cells (in vivo) B16 and HepG2 B16F10 (in vivo) SKOV-3 cells and MDA-MB-231 cells (in vivo)	[35] [36] [37] [38] [39]
HA/Tf <i>dual targeting with Transferrin (Tf)</i>	CD44/TfR	lipid carriers	A549 (in vivo)	[40]
Tf/TGF α Tf/mAb2C5 Tf/FA Tf/Tet-1 Tf/EGF	TfR/EGF receptor TfR/nucleosomes TfR/FR TfR/ganglioside GT1 B receptor TfR/EGFR	polyplexes micelles liposomes polymersomes silica nanoparticles	A549 and CHO-K1 cells A2780 (in vivo) C6 glioma cells (in vivo) bEnd.3 and Neuro-2a cells (in vivo) HEK-293 cells	[41] [42] [43] [44] [45]
<i>Other dual molecular targeting</i>				
FA/mAb225 FA/TPP AS1411/TGN peptide AS1411/TGN peptide Angiopep-2 /tLyP-1 biotin/HMGB1 tLyP-1/Lf	FR/EGFR FR/mitochondria nucleolin/TGN receptor nucleolin/TGN receptor LRP/neuropilin-1 biotin receptor/nuclear targeting NRP-1/Lf receptor	liposomes pro-apoptotic peptide PEG-PCL nanoparticles PEG-PCL nanoparticles liposomes PAMAM PEG-PLA nanoparticles	KB cells KB cells C6 glioma cells (in vivo) C6 glioma cells (in vivo) U87MG (in vivo) COS7 cells C6 glioma cells (in vivo)	[46] [47] [48] [49] [50] [51] [52]
Targeting combined with cell penetrating peptides				
RGD/TAT	$\alpha_v\beta_3$ integrin/cell membrane	PAMAM quantum dot polymeric micelles liposomes mesoporous silica nanoparticles	MCF-7 (in vivo) U87MG cells MDA435/LCC6 resistant cells HepG2 and Hela cells (in vivo) HeLa (in vivo)	[53] [54] [55] [56] [57]
RGD/R8	$\alpha_v\beta_3$ integrin/cell membrane	liposomes lipopeptides	HUVEC cells HeLa cells	[58] [59]
NGR/STR-R4 NGR/R4 NGR/CPP Tf/TAT	CD13/cell membrane CD13/cell membrane CD13/cell membrane TfR/cell membrane	liposomes liposomes liposomes liposomes	MS-1 and TE cells OS-RC-2 cells (in vivo) HT-1080 cells HepG2 (in vivo)	[60] [61] [62] [63]
Angiopep-2/R8 CCK8/R8	LRP/cell membrane cholecystokinin receptors/cell membrane	micelles liposomes	C6 glioma cells (in vivo) A431 cells	[64] [65] [66]
T7/TAT Galactose/TAT Aptamer/R8	TfR/cell membrane galactose receptor/cell membrane mitochondrial outer membrane/cell membrane	liposomes nanocomplexes liposomes	C6 glioma (in vivo) QGY-7703 (in vivo) HeLa (in vivo)	[67] [68] [69]
FA/TAT mAb 2C5/TAT	FR/cell membrane nucleosomes/cell membrane	liposomes liposomes	KB cells 4T1 cells B16-F10, MCF-7 and HeLa cells	[70] [71] [72]
Dual-targeting with one ligand				
cRGD	$\alpha_v\beta_3$ integrin on neovascular and tumor cells	PAMAM	HUVEC and B16 cells (in vivo)	[73]
PHSCNK	$\alpha_5\beta_1$ integrin on neovascular and tumor cells	liposomes	HUVEC and MDA-MB-231 cells	[74]
tLyP-1	neuropilin (NRP) on neovascular and tumor cells	mesoporous silica nanoparticles	HUVEC and MDA-MB-231 cells	[75]
EGFP-EGF1 (ENP)	tissue factor (TF) on neovascular and glioma cells	PEG-PLA nanoparticles	HUVEC and C6 glioma cells (in vivo)	[76]
Angiopep-2	low-density lipoprotein receptor-related protein (LRP) on BBB and glioblastoma cells	upconversion nanoparticles PEG-PCL nanoparticles liposomes carbon nanotubes PAMAM	BCECs and U87MG glioma cells (in vivo) BCECs and U87MG glioma cells (in vivo) BCECs and U87MG glioma cells (in vivo) BCECs and C6 glioma cells (in vivo) C6 glioma cells (in vivo)	[77] [78] [79] [80] [81]

Table 1 (Continued)

Dual-ligand strategies	Targets	Carrier	Cancer Model	Ref.
peptide-22 apolipoprotein E (ApoE)	LRP on BBB and glioblastoma cells LRP on BBB and glioblastoma cells	PEG-PLA Nanoparticle nanodisk ApoE-based nanoparticles	BCECs and C6 glioma cells (in vivo) SF-763 and SF-767 glioma cells C6 glioma cells	[82] [83] [84]
lactoferrin (Lf)	lactoferrin receptor (Lfr) on BBB and glioblastoma cells	liposomes polymerosomes magnetic nanogels superparamagnetic iron oxide nanoparticles BSA nanoparticles PEG-PLA-resveratrol conjugates PCL-PPE and PEG-PCL hybrid micelle magnetic silica PLGA nanoparticles nanoscaled graphene oxide	BCECs and C6 glioma cells (in vivo) C6 glioma cells (in vivo) C6 glioma cells (in vivo MRI) C6 glioma cells (in vivo MRI)	[85] [86] [87] [88]
Tf	TfR on BBB and glioblastoma cells	BCECs and C6 glioma cells (in vivo) U87MG and C6 cells (in vivo)	[89] [90]	
HA	CD44 on breast cancer cells and stem cells	bEnd.3 and U87MG (in vivo) C6 cells (in vivo) MCF-7 cancer stem cells and MDA-MB-231 metastatic breast cancer cells HA-SS-PLGA	[91] [92] [93] [94] [95]	

et al. constructed anginex (Anx) and cyclic RGD peptide (RGD) co-modified paramagnetic liposomes (Anx/RGD-L), which respectively target galectin-1 and $\alpha_v\beta_3$ integrin on activated endothelial cells (Fig. 1) [25]. Anx/RGD-L significantly enhanced the cellular uptake of liposomes, leading to better magnetic resonance imaging (MRI) and inhibition effects for angiogenesis in vitro as compared to single ligand targeting. In addition, it was found that Anx/RGD-L liposomes with high ligand density performed better than liposomes with low ligand density. Interestingly, the improvement found with the use of a high ligand density is in contrast with the results obtained by Laginha et al. who prepared doxorubicin-loaded liposomes decorated with two different antibodies, α CD19 and α CD20 for human B lymphoma cell targeting [101]. They pointed out that a high density of antibodies on the surface of the liposomes may cause steric hindrance for binding to the receptor of cells or produce multivalent binding, where one liposome binds to two or more antigens, therefore decreasing the cellular uptake efficiency. Kluza et al. stated that the different results in their study as compared to those of Laginha et al. may probably be explained by the relatively low molecular weights of Anx (4 kDa) and RGD (0.72 kDa) as compared to those of antibodies (150 kDa), reducing the interaction between the ligands used [25]. Importantly, a synergistic effect was observed when using Anx/RGD-L co-modified liposomes while only an additive effect was shown using mixtures of Anx-L and RGD-L liposomes, confirming the importance of dual-ligand targeting. Based on these promising results in vitro, Kluza et al. applied Anx/RGD-L for angiogenesis-specific MRI in subcutaneous B16F10 melanoma-bearing mice [26]. The dual-targeting with Anx/RGD-L displayed enhanced specificity for B16F10 melanoma endothelium which is crucial in MRI imaging, while it was noticed that the targeting efficacy of Anx/RGD-L for tumor tissue was lower than that of RGD-L, probably because the high density of positively-charged Anx facilitated the clearance of liposomes from the blood. These results reveal that in vivo targeted delivery of dual-targeted nanocarriers is much more complicated than that in vitro, and importantly, the in vivo stability (including blood circulation times) of nanocarriers has great impact on their targeting properties. The synergistic effect of dual targeting was also observed in prostate cancer gene therapy by RGD and B6 co-functionalized polyplexes [27]. By simultaneous recognition of $\alpha_v\beta_3$ integrin and transferrin receptors (TfR) on prostate cells, the transfection efficiency of dual targeting polyplexes was 60-fold and 20 fold higher in DU145 and PC3 prostate cancer cells, respectively, than that of pegylated polyplexes. The less pronounced transfection efficiency in PC3 cells

is probably due to the moderate expression of integrin receptors, indicating that the density of receptors also plays an important role in targeting. Importantly, it was suggested that the reason why dual-targeting polyplexes exhibited better transfection efficiency than the mixture of two single-targeting polyplexes is probably the synergistic binding of RGD and B6 to their respective receptors to mediate a more efficient uptake (cellular association is mediated largely by RGD-integrin binding, whereas uptake is predominantly proceeding via TfR mediated endocytosis). Besides based on in vitro results, in vivo targeted delivery by estrone (targeting estrogen receptor, ER) and RGD peptide co-modified hydrogel which can self-assemble into short nanofibers with a width of 20 nm demonstrated a preferential accumulation in a subcutaneous MCF-7 breast tumor of mice (ER and $\alpha_v\beta_3$ integrin overexpressing) [33].

As is known, angiogenesis is one of the main features in tumor development, providing nutrition to tumor cells for growth, invasiveness and metastasis. Therefore, simultaneous targeting of neovascular cells and tumor cells attracts great interest to achieve better antitumor efficacy. Xu et al. prepared paclitaxel (PTX)-loaded nanoparticles (NPs) decorated with RGD and transferrin (TF) to respectively target human umbilical vein endothelial cells (HUVECs) and human cervical carcinoma (HeLa) cells, revealing faster and greater uptake of dual-targeting nanoparticles compared to non-targeted nanoparticles, leading to higher cytotoxicity in both cells (Fig. 2) [28]. Different from the first type of dual-targeting, no synergistic effect in cellular uptake was found using RGD-Tf-NPs compared with RGD-NPs in HUVECs cells ($\alpha_v\beta_3^+TfR^-$) or Tf-NPs in HeLa cells ($\alpha_v\beta_3^-TfR^+$), but a comprehensive effect from targeting both cells was achieved, which is also an effective approach in tumor therapy. Moreover, by combining the first and second type of dual targeting, interleukin-13 (IL-13) and RGD co-functionalized polymeric nanoparticles (IRNPs) displayed both strong targeting to HUVEC cells ($\alpha_v\beta_3^+ IL13R\alpha2^-$) and C6 glioma cells ($\alpha_v\beta_3^+ IL13R\alpha2^+$) [29]. Using IRNPs loaded with the cytotoxic agent docetaxel (DTX) in orthotopic C6 glioma-bearing mice led to significant longer survival times than the use of single-targeting nanoparticles [30].

Another type of dual-targeting with RGD focuses both on cellular and subcellular levels. Han et al. constructed a chimeric peptide containing the Arg-Gly-Asp-Ser (RGDS) peptide sequence as the tumor targeting ligand and the D₂(KLAKLAK)₂ peptide sequence as a mitochondrion targeting ligand as well as an executioner [32]. After the first step of receptor-mediated endocytosis via the interaction of cRGD and $\alpha_v\beta_3$ integrins of U87MG cells, the second step

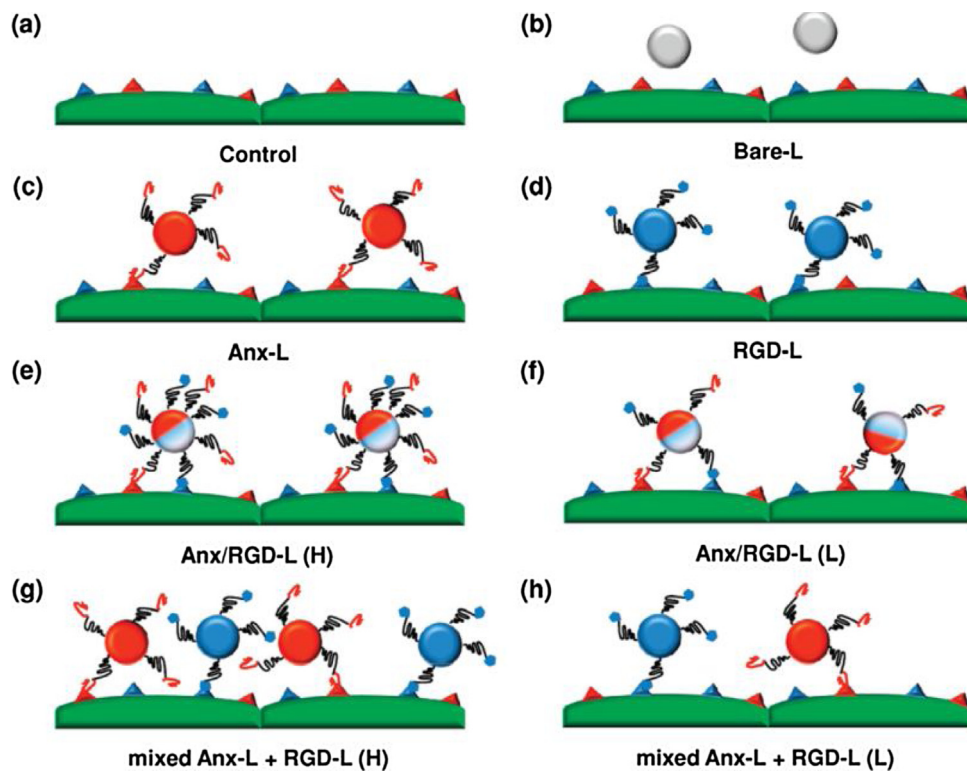


Fig. 1. Schematic representation of the experimental setup for the study of Anx and RGD dual-targeting effect. Efficacy of the cellular uptake has been investigated for the following conditions: (a) culture medium (Control), (b) nontargeted liposomes (Bare-L), (c) Anx-conjugated liposomes (Anx-L), (d) RGD-conjugated liposomes (RGD-L), (e) Anx and RGD dual-conjugated liposomes containing high concentration of peptides [Anx/RGD-L (H)], (f) Anx and RGD dual-conjugated liposomes containing low concentration of peptides [Anx/RGD-L (L)], (g) mixture of Anx-L and RGD-L containing high concentration of peptides [mixed Anx-L+RGD-L (H)], and (h) mixture of Anx-L and RGD-L containing low concentration of peptides [mixed Anx-L+RGD-L (L)]. The figure was inspired by Laginha K et al. [101]. Images reproduced from [25] with permission from the American Chemical Society, Copyright 2010.

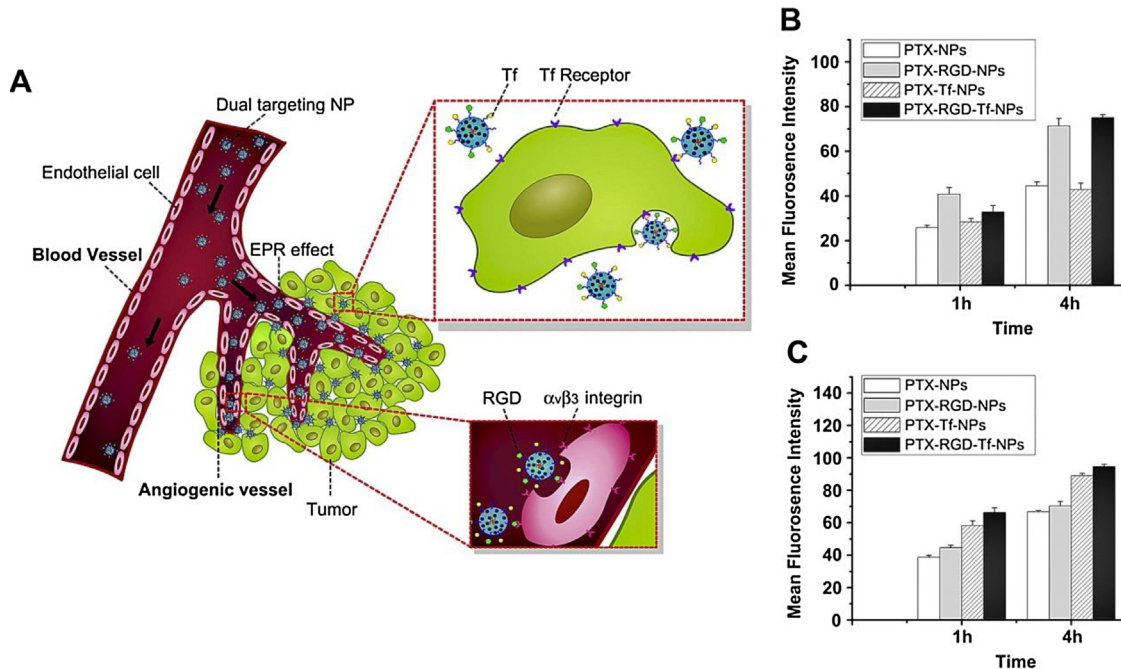


Fig. 2. (A) Schematic representation of the mechanisms by which dual-targeting nanocarriers can deliver PTX to tumor tissues. Passive targeting is achieved by extravasation of NPs through the enhanced permeability of the tumor vasculature (EPR effect). Active tumor targeting can be achieved by decoration of nanocarriers with RGD and Tf that promote cell-specific recognition and binding. The ligand RGD enhances the targeting migration and accumulation of NPs to the $\alpha\beta_3$ integrin-expressing tumor vasculature and Tf then improves the cellular uptake of NPs by TfR expressing tumor cells. The cellular uptake of different PTX formulations in HUVECs (B) and HeLa cells (C) at 250 mg/mL after 1 h and 4 h incubation expressed as geometric mean fluorescence intensity ($n = 3$). Images reproduced from [28] with permission from Elsevier, Copyright 2011.

involves the targeting of mitochondria by D(KLAKLAK)₂ peptide and subsequent disruption of mitochondrial membranes, inducing apoptosis of tumor cells. Besides mitochondria, nuclei of tumor cells are another important subcellular target. Aptamer AS1411, which has a high affinity to nucleolin, was co-conjugated to a gold nanocluster-DOX prodrug together with cRGD (AuNC-DOX-cRGD-Apt) (Fig. 3) [34]. Notably, both efficient cellular uptake as well as nuclear distribution of the prodrug was observed in U87MG cells ($\alpha_v\beta_3$ and nucleolin positive) after short time incubation, leading to better antitumor efficacy compared to AuNC-DOX-cRGD in U87MG tumor-bearing mice. This strategy combines both cell membrane targeting and subcellular compartment targeting, enabling nanomedicines to act more precisely on tumor cells. The above examples all demonstrate the advantages obtained with nanosystems containing RGD and another ligand for dual targeting. Nevertheless, Rangger et al. reported that even no additive effect was found when using RGD ($\alpha_v\beta_3$ targeting) and substance P (SP, neurokinin-1 targeting) co-functionalized liposomes (Hybrid-LPs) for targeted delivery and imaging both in vitro and in vivo [31]. The in vitro cellular uptake study showed good binding of single-targeting RGD-LPs to both human melanoma M21 cells ($\alpha_v\beta_3^+$ neurokinin-1 $^-$) and human glioma U87MG cells ($\alpha_v\beta_3^+$ neurokinin-1 $^+$), and also good binding of single-targeting SP-LPs to U87MG cells, demonstrating the specific targeting effect of either single ligand. However, no improvement of cellular uptake was found using the Hybrid-LPs, implying that some problems (such as ligand density and interactions between ligands) may exist in the combination of the two kinds of ligands. Weak targeting effects of nanocarriers in vitro very likely leads to bad performance in vivo as the in vivo environment is much more complex. Therefore, the arrangement of the two ligands including position and density is a crucial issue to be considered when designing dual-targeting nanocarriers, and it is also important to confirm the dual-targeting effect firstly in vitro.

Dual targeting with HA

Hyaluronic acid (HA), is a natural acidic polysaccharide macromolecule composed of N-acetylglucosamine and D-glucuronic acid disaccharide units present in the extracellular matrix and synovial fluids. Owing to its biocompatibility and biodegradability, HA has been extensively investigated for biomedical applications. In particular, HA can specifically bind to cluster determinant 44 (CD44) that are overexpressed on various cancer cells, enabling broad applications of HA-based nanomedicines in tumor therapy [102–105]. Therefore, dual-targeting with HA also became attractive to achieve better efficacy. Generally, dual-targeting with HA can be divided into two categories according to the conjugation methods. The most commonly used modification method is conjugating another targeting molecule to the HA chain, which has an abundance of functional groups. Liu et al. constructed FA and HA dual-targeting micelles by conjugating FA to the $-\text{CH}_2\text{OH}$ groups of HA (MW = 11 kDa)-octadecyl (HA-C₁₈) (Fig. 4) [35]. In A549 lung cancer cells (FR $^+$ CD44 $^+$), FA-HA-C₁₈ micelles exhibited similar effects in cellular uptake as compared to HA micelles. In contrast in MCF-7 breast cancer cells (FR $^+$ CD44 $^+$), more cellular uptake of FA-HA-C₁₈ micelles was found than the uptake of HA micelles after 2 h incubation, due to concurrent interaction of the ligands with the folate and CD44 receptors on the surface of MCF-7 cells. In addition, multiple endocytosis pathways are involved in the cellular uptake of FA-HA-C₁₈ micelles in MCF-7 cells [35]. Based on this study, Liu et al. applied PTX-loaded FA-HA-C₁₈ micelles to overcome the multidrug resistance in MCF-7/Adr breast cancer since efficient intracellular uptake of drug may avoid P-glycoprotein (P-gp)-mediated drug efflux [36]. It was found that PTX-loaded FA-HA-C₁₈ micelles displayed a better MDR reversal effect in MCF-

7/Adr cells and also improved PTX distribution in tumor tissues in MCF-7 breast tumor-bearing mice compared with the use of PTX loaded single-targeting HA micelles, probably because FA and CD44 receptor dual targeting leads to more efficient cellular uptake. In another example, tetraiodothyroacetic acid (tetrac), a specific ligand of $\alpha_v\beta_3$, was conjugated to HA (~58 kDa) via an amidation reaction to achieve a dual-targeting effect [38]. DTX-loaded tetrac-HA co-modified solid lipid nanoparticles (TeHA-SLN) exhibited synergistic targeting to both tumor blood vessels and tumor cells, resulting in a stronger tumor inhibition effect than obtained with the use of DTX-loaded Te-SLN or HA-SLN in both a B16F10 ($\alpha_v\beta_3^+/\text{CD44}^+$) melanoma subcutaneous mice model as well as in an in situ lung metastasis mice model. Interestingly, MCF-7 breast cancer cells were used as $\alpha_v\beta_3^-/\text{CD44}^-$ negative control cells here. The inconsistency in the two studies above with respect to the properties of MCF-7 breast cancer cells reveals that firstly the expressed amount of receptors on tumor cells may vary depending on the reference cell line used and secondly, the amount and type of receptors expressed on tumor cells are not constant. Even in the same cell line, the receptors may vary due to different cell origins, in vitro culture methods and time, in vivo tumor progress, etc. Therefore, besides referring to papers in the literature, it is necessary to determine the expression of specific receptors in a cell line before these are used for uptake studies. However, the expression of receptors on cells in vivo is still difficult to monitor due to the complex tumor environment. Therefore, using a dual targeting strategy may decrease the uncertainties involved in single-ligand targeting. Besides small molecules, peptides can also be conjugated to HA to achieve synergistic effects. In the study of Chen et al., GE11 peptide (YHWYGYTPQNVI), which has a high affinity to epidermal growth factor receptor (EGFR), was conjugated to HA via an amidation reaction [39]. The uptake of nanogels with an optimal molar ratio of GE11 to HA by CD44 and EGFR-positive SKOV-3 ovarian cancer cells was significantly increased as compared to the uptake of HA nanogels. After loading with apoptosis-inducing protein Granzyme B, the GE11/HA nanogels almost completely inhibited the tumor growth in both CD44 and EGFR-positive SKOV-3 human ovarian carcinoma and MDA-MB-231 human breast tumor bearing mice, which signifies the important role of dual targeting in tumor-targeted therapy.

Besides being conjugated to HA, another ligand and HA can also be attached separately onto a single nano-system. To efficiently deliver genes to A549 lung cancer cells (TFR $^+$ CD44 $^+$), transferrin and HA (5 kDa) were both conjugated to PEG-DSPE for the decoration of a cationic liposomal system (Fig. 5) [40]. Single-ligand modified liposomes (TF liposomes or HA liposomes) had similar gene transfection efficiencies, while dual-targeting liposomes exhibited a much higher gene transfection capacity both in vitro and in vivo (A549 lung cancer-bearing nude mice). HA can also be decorated onto positively-charged nanocarriers by electrostatic interaction because of abundant negatively charged carboxyl groups in its structure. Applying this method, FA and HA (300 kDa) dual-targeting liposomes based on PEI were developed for simultaneous delivery of PTX and DNA to CD44-positive and FR-positive B16 cells (Fig. 6) [37]. Compared with FA modified liposomes, further modification with HA could efficiently prevent aggregation of positively-charged liposomes in plasma and also protect DNA from degradation by DNase, leading to significantly improved transfection efficacy and enhanced cellular uptake.

The studies above reveal that the synergistic effect of different ligands and HA can be achieved in various ways. However, the systems to be used should be studied in more detail to achieve better targeting effects. As is known, carboxyl groups of HA are the recognition sites for HA receptors and hyaluronidase. Slight modification of the carboxyl groups of HA (less than 25 mol%) retains the high affinity of HA for its receptors, while with more extensive modifica-

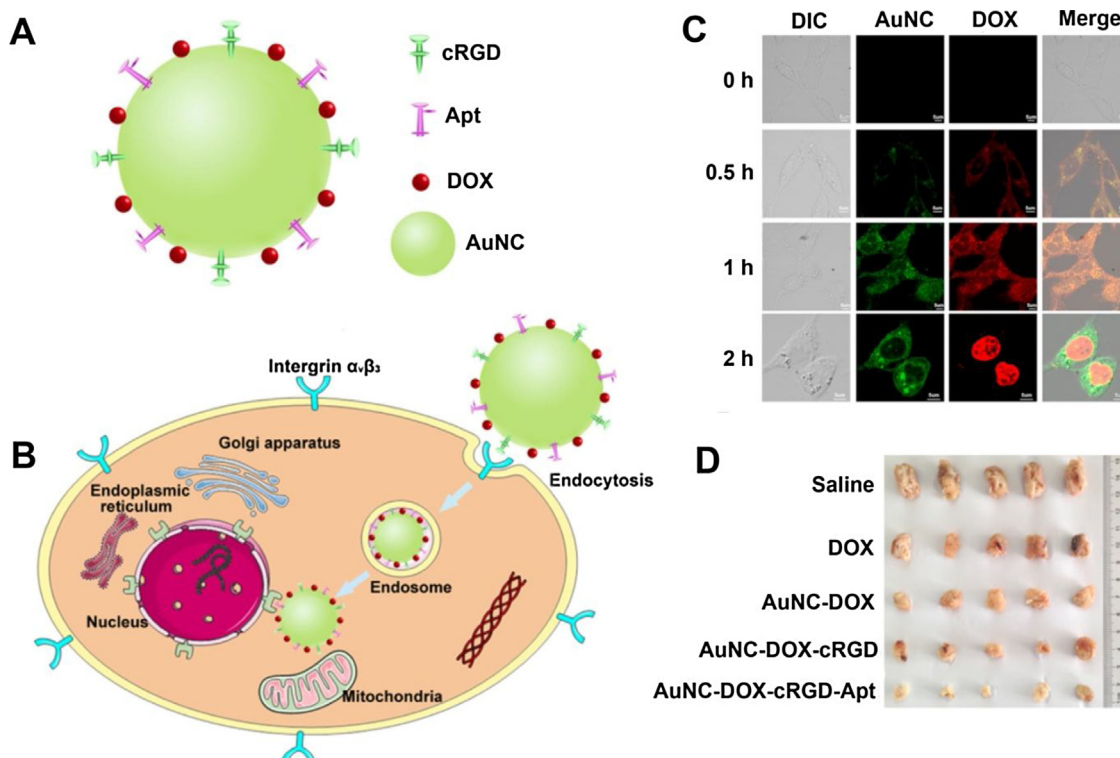


Fig. 3. (A) Schematic nanostructure of AuNC-DOX-cRGD-Apt, (B) Schematic illustration of the endocytosis process of AuNC-DOX-cRGD-Apt in U87MG cell lines monitored by confocal microscopy and (D) tumor images isolated from tumor-bearing mice after treatment with saline, free DOX, AuNC-DOX, AuNC-DOX-cRGD and AuNC-DOX-cRGD-Apt. Images reproduced from [34] with permission from Elsevier, Copyright 2016.

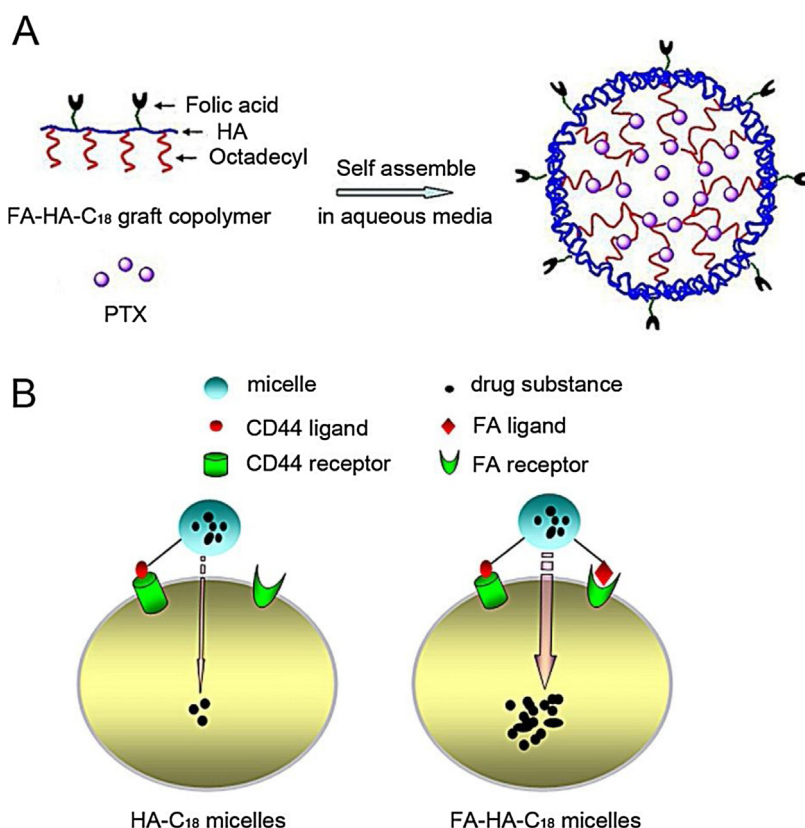


Fig. 4. Schematic representations for (A) the self-assembling and drug-loading mechanisms of polymeric micelles from FA-HA-C₁₈ graft copolymer in aqueous solution and (B) targeting mechanism of HA-C₁₈ micelles (A) and FA-HA-C₁₈ micelles. Images reproduced from [35] with permission from Elsevier, Copyright 2011.

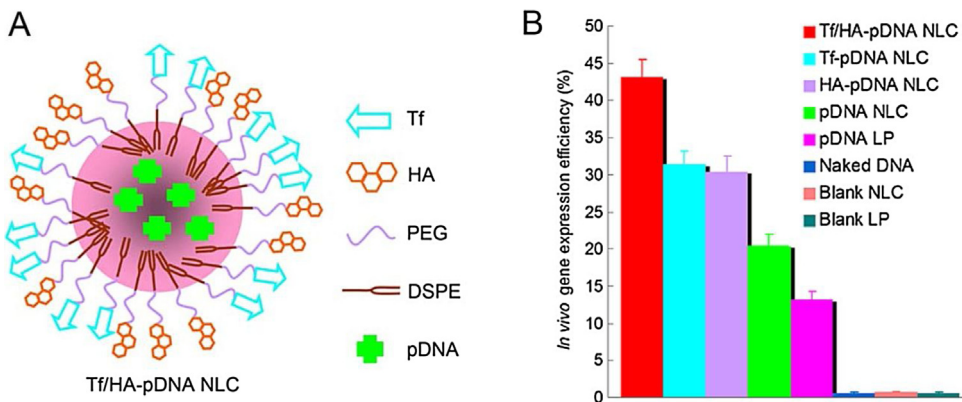


Fig. 5. (A) Composition diagram of Tf/HA-pDNA NLC and (B) *In vivo* gene expression results of different systems used for lung cancer bearing mice. Images reproduced from [40] with permission from Spandidos Publications, Copyright 2017.

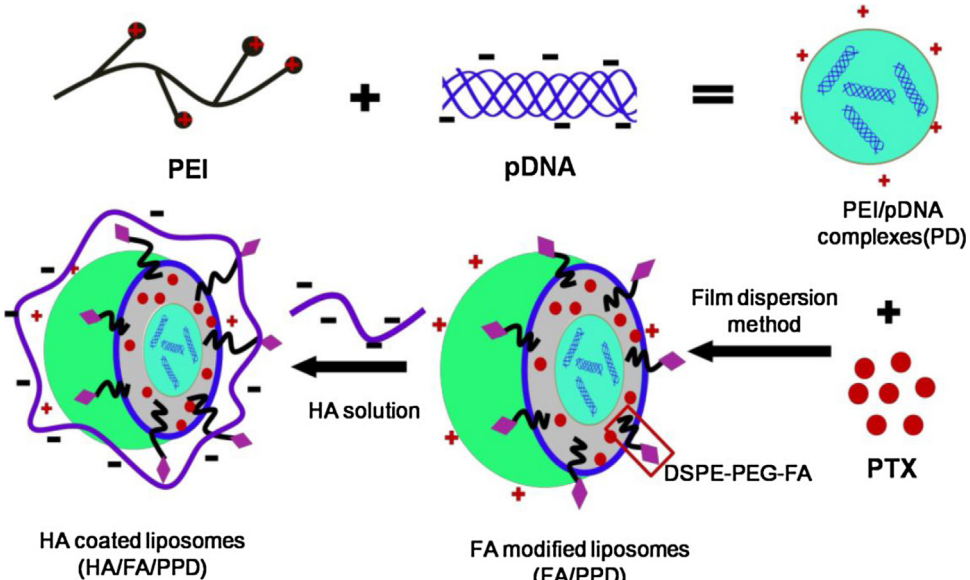


Fig. 6. Schematic illustration of the formation of HA/FA/PPD (hyaluronic acid (HA) and folate (FA)-modified liposomes). Firstly, PEI (polyethyleneimine) binds DNA to form the condensed cationic PEI/DNA complexes, which were chosen as the cationic core of the liposomes. Subsequently, PTX (paclitaxel) and PEI/DNA complexes were co-loaded in DSPE-PEG2000-FA-modified liposomes, forming the FA-modified cationic liposomes (FA/PPD). Lastly, the cationic FA/PPD was added to the anionic HA solution to obtain the HA coated FA/PPD (HA/FA/PPD) by electrostatic attraction. Images reproduced from [37], open access publication.

tion, the targeting efficiency of HA may be reduced [106]. Another problem is that ligands may be partially shielded when conjugated to the HA chain due to the random coil conformation of HA when extending in the solution, resulting in a decreased effective surface density of the second ligand. The shielding effect of HA may also be present when ligands and HA are separately decorated on the same nanocarrier because of the high molecular weight of HA, or when HA is wrapped around nanocarriers. These issues should be considered in designing dual-targeting nanomedicines with HA and other ligands to achieve improved targeting effects.

Dual targeting with transferrin

Transferrin (Tf) is a serum glycoprotein that helps transporting iron through the blood and into cells by binding to the transferrin receptor (TfR) followed by internalization via receptor-mediated endocytosis [6]. The transferrin receptor is overexpressed in malignant tumor cells (may be up to 100-fold higher than the average expression on normal cells) due to the increased requirement of iron [3], making this receptor attractive for tumor targeting, while

dual targeting with transferrin is also expected to achieve better targeting effects.

Kakimoto et al. introduced Tf and transforming growth factor alpha (TGF α) onto a polyethyleneimine polyplex (Tf&TGF α -polyplex) for efficient and specific gene delivery [41]. Optimized Tf and TGF α densities significantly enhanced the transfection efficiency of the polyplex as compared to single-targeted Tf-polyplex or TGF α -polyplex in A549 lung cancer cells (TfR $^+$ EGFR $^+$). Interestingly, the transfection efficiency of Tf- and TGF α -polyplex was almost equal although the expression of the TfR was more apparent than that of EGFR in A549 cells, probably because TGF α had a higher affinity to EGFR than Tf to its receptors. It has also been noticed that although TfR is overexpressed on Chinese hamster ovary CHO-K1 cells, no Tf receptor-mediated endocytosis was observed, probably due to the structural differences of transferrin receptors in Chinese hamsters from that in humans resulting in low affinity with human transferrin, indicating the specificity of ligand-receptor binding. This study also revealed that ligand density, affinity and specificity for receptors are all important factors that may affect targeting efficacy. However, because of the complicated tumor environment and altered blood flow in tumors these factors have to be optimized

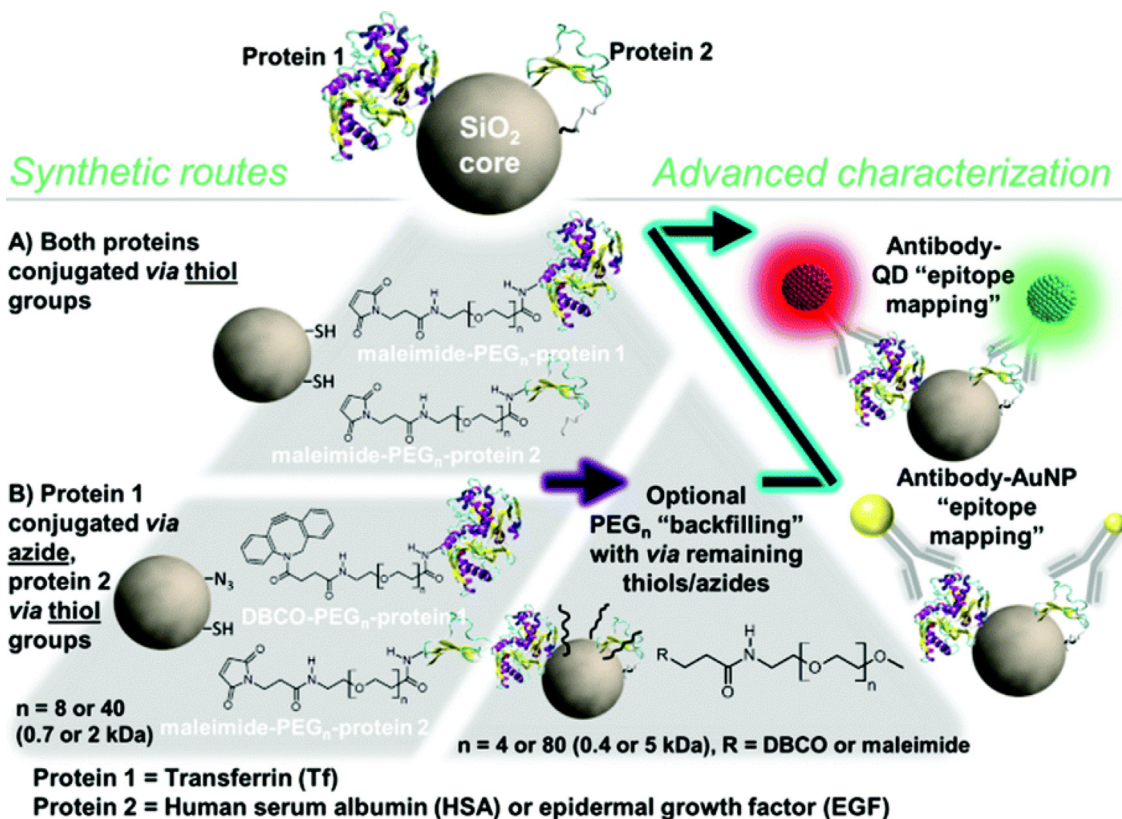


Fig. 7. Synthetic strategies used to obtain bifunctional NP-protein conjugates and illustration of their characterization with nanoprobes. Images reproduced from [45] with permission from the Royal Society of Chemistry, Copyright 2016.

in order to achieve satisfactory *in vivo* targeted delivery. Sawant et al. designed Tf and mAb monoclonal antibody (mAb) 2C5 modified polyethylene glycol-phosphatidylethanolamine (mPEG-PE) micelles for efficient targeted delivery of a poor soluble drug, R547 (a selective adenosine triphosphate-competitive cyclin-dependent kinase inhibitor) to A2780 ovarian carcinoma *in vitro* and *in vivo* [42]. With optimized ligand density of Tf and (mAb) 2C5, significantly enhanced cellular uptake and cytotoxicity in A2780 cells were observed compared to single ligand-targeted micelles. However, the antitumor efficacy of R547-loaded dual-targeting micelles in subcutaneous A2780 ovarian carcinoma bearing mice was even weaker than that of single-targeting Tf-micelles. The authors gave two possible reasons to explain this phenomenon. Firstly, steric hindrance caused by the bulky structure of mAb 2C5 along with that of Tf limits the cellular uptake *in vivo*. Secondly, the efficiency of the EPR effect is the rate-limiting step *in vivo* for the uptake and accumulation of R547-loaded micelles in the tumors. Besides these two reasons, short circulation times due to dual-ligand modification [26] and rapid liver uptake of these small sized micelles (13–16 nm) [107] may also be important factors resulting in low efficacy *in vivo*.

Since TfR is also overexpressed on brain endothelial cells, numerous studies have demonstrated that Tf-modified nanocarriers showed efficient BBB permeation. To simultaneously achieve transport across the BBB and glioma targeting, Gao et al. prepared Tf and folate (F) dual-targeting DOX-loaded liposomes [43]. It was demonstrated that Tf modification can inhibit the BBB p-gp efflux of DOX due to receptor-mediated endocytosis. Surprisingly, dual-targeting liposomes had a significantly higher transport ratio across the BBB than Tf-liposomes, while there was no evidence that folate ligands can help to cross the BBB. An *in vivo* study showed that the dual-targeting DOX-loaded liposomes had better anti-glioma efficacy compared to non-targeted DOX-loaded liposomes in ortho-

topic C6 glioma-bearing mice. However, in this study the possible advantages of the dual-targeting strategy have not been clearly illustrated, because single-targeted liposomes were not used as controls and sometimes single-targeting may perform better than dual-targeting in the complex *in vivo* environment as demonstrated in Sawantis work [42]. In addition to brain endothelial cells, TfRs are also found on the plasma membrane of neurons, which, in principle, provides the possibility to target neurons with Tf-modified nanomedicine to cure neurodegenerative diseases such as Alzheimer's disease (AD) [44]. Tet-1 is a 12-amino acid peptide which has high affinity to GT1B receptor on the neurons. Combining the advantages of Tf and Tet-1, significantly higher brain permeation and uptake was found using Tf and Tet-1 dual-targeting PEG-PLGA polymersomes (Tf/Tet-1-POS) than single-targeting Tf-POS or Tet-1-POS. After loading curcumin, which can bind to amyloid β (A β) protein, promoting the degradation of deposited plaques and reducing A β -induced neurotoxicity, Tf/Tet-1-POS significantly ameliorated cognitive dysfunction induced by A β_{1-42} in mice as compared to curcumin-loaded Tf-POS or Tet-1-POS.

Although improved cellular uptake *in vitro* or *in vivo* was found using the dual-targeting strategy with transferrin in the studies above, various factors such as particle size, ligand density, ligand specificity and affinity for receptors may still affect the targeting efficiency of dual-ligand targeting nanomedicine. Generally, the information about these factors has been indirectly obtained by *in vitro* or *in vivo* experiments and the exact reasons for poor targeting remain unclear since the activities of targeting ligands after being conjugated to nanocarriers, especially those of proteins with more complicated structures than small molecules, are usually unknown. Addressing this problem, Giudice et al. optimized the construction of Tf-HSA or Tf-EGF bifunctional fluorescent silica NPs by using different conjugation strategies and also developed a highly sensitive method that enables simulta-

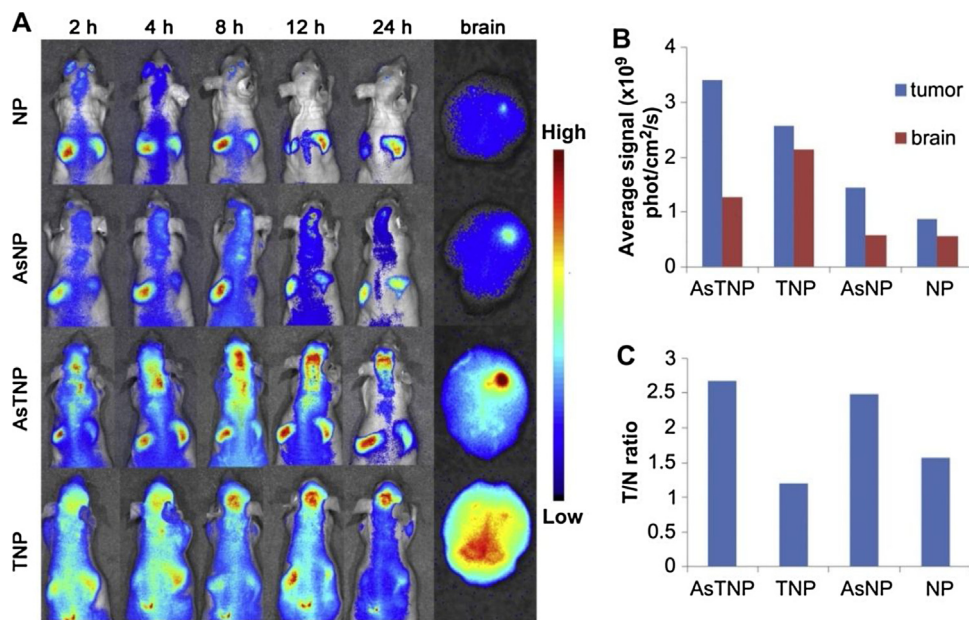


Fig. 8. (A) The in vivo imaging of DiR-loaded NP, AsNP, AsTNP and TNP in brain glioma bearing nude mice at several time points with ex vivo imaging of the brain at 24 h. (B) Brain and glioma fluorescence intensity at 24 h. (C) The fluorescent intensity ratio of tumor/normal brain (T/N ratio) of the brains 24 h after treatment with different formulations. Images reproduced from [48] with permission from Elsevier, Copyright 2012.

neous *in situ* detection of two surface motifs on the bifunctional NP-protein conjugates [45]. In their study, the maleimide-thiol reaction and azide-dibenzocyclooctyl (DBCO) click reaction were employed to conjugate different proteins to the NPs as shown in Fig. 7. Surprisingly, excess non-specifically bound protein was found after using both conjugating strategies as determined by sodium dodecyl sulfate polyacrylamide gel electrophoresis (SDS-PAGE) analysis. Non-specifically bound proteins after conjugation are usually ignored. However, they may greatly influence the targeting efficacy as they may be exchanged by other proteins in the biological milieu leading to unpredictable behavior or binding to the receptors resulting in poor uptake of nanocarriers. Fortunately, backfilling with PEG (MW = 5 kDa) of the silica NPs greatly reduced the amount of non-specifically bound proteins due to displacement by PEG molecules. Moreover, simultaneous detection of the two surface motifs on the bifunctional NP-protein conjugates was available by using antibody-conjugated, immune quantum dots (QDs) nanoprobes and fluorescence spectrometric analysis. This analysis indicated that only 17% of the grafted Tf and 0.6% of the EGF were recognizable by the nanoprobes probably due to shielding with the long PEG. Noticeably, less EGF was probed than Tf, while the number of bound EGF molecules was higher, probably because some EGF molecules are buried within neighboring large sized Tf or long PEG molecules. Therefore, simultaneous analysis of dual-targeting nanocarriers regarding the binding of non-specific ligands and the surface concentration of recognizable ligands may provide a better insight for optimizing dual-targeting nanomedicine. In addition, the modification of nanocarriers with ligands combined with PEGylation has to be balanced to achieve optimal targeting effects.

Other dual molecular targeting

Besides dual-molecular targeting in combination with either RGD, HA or transferrin, miscellaneous dual-molecular targeted nanomedicines have been developed. Glioma-targeting is one of the most important applications of dual molecular targeting. The strategy for the use of nanomedicines for glioma treatment usually includes two aspects, i.e. transporting the nanosystem across the blood-brain barrier (BBB) and targeting to the glioma cells.

Receptor-mediated transcytosis by brain endothelial cells is a classical mechanism for nanomedicines to permeate the BBB [108]. Therefore nanomedicines with dual molecular targeting, which respectively target brain endothelial cells and glioma cells, have great potential for effective glioma therapy. A cascade delivery strategy was developed by introducing TGN peptide and AS1411 aptamer on DTX-loaded PEG-PCL nanoparticles (AsTNP) [48]. TGN is a 12-amino acid peptide that has been obtained by *in vivo* phage display screening from a 12-mer peptide library. It has been demonstrated that TGN can facilitate BBB targeting and accumulate more particles in the brain compared to unmodified particles. AS1411 is a G-rich DNA aptamer, which specifically binds to nucleolin overexpressed on C6 glioma cells. By sequential BBB targeting and permeation of the BBB by the use of TGN and glioma targeting and penetration by AS1411, these dual-targeted nanoparticles could be used both for precise glioma imaging and effective glioma therapy (Fig. 8). Although *in vivo* imaging showed that the brain fluorescence signal intensity of single-targeting TGN modified nanoparticles (TNP) was much higher than that of non-targeted NP, the non-selective distribution in the brain resulted in poor glioma imaging. On the other hand, single-targeting AS1411 modified nanoparticles (AsNP) exhibited better glioma imaging but a lower fluorescence signal intensity than TNP due to poor BBB permeation. Therefore, both BBB and glioma targeting are required in glioma therapy. Considering that the orthotopic glioma model is difficult to establish, building *in vitro* models that mimic the microenvironment of glioma is of great importance to evaluate the glioma targeting efficacy of nanomedicine before carrying out *in vivo* experiments. Since it has been demonstrated that DTX-loaded AsTNP are effective in glioma therapy *in vivo* [48], it seems a good system for the evaluation of the performance of *in vitro* models. Traditional cellular uptake and cytotoxicity studies in glioma therapy are usually directly carried out on brain endothelial cells or glioma cells, whereas the *in vivo* glioma microenvironment is quite different. Therefore, Gao et al. developed *in vitro* evaluation models in which cellular uptake and cytotoxicity studies of DTX-loaded AsTNP were performed in a system in which the nanocarriers first had to pass a bEnd.3 brain endothelial cell monolayer before reaching the glioma cells [49]. Major differences were

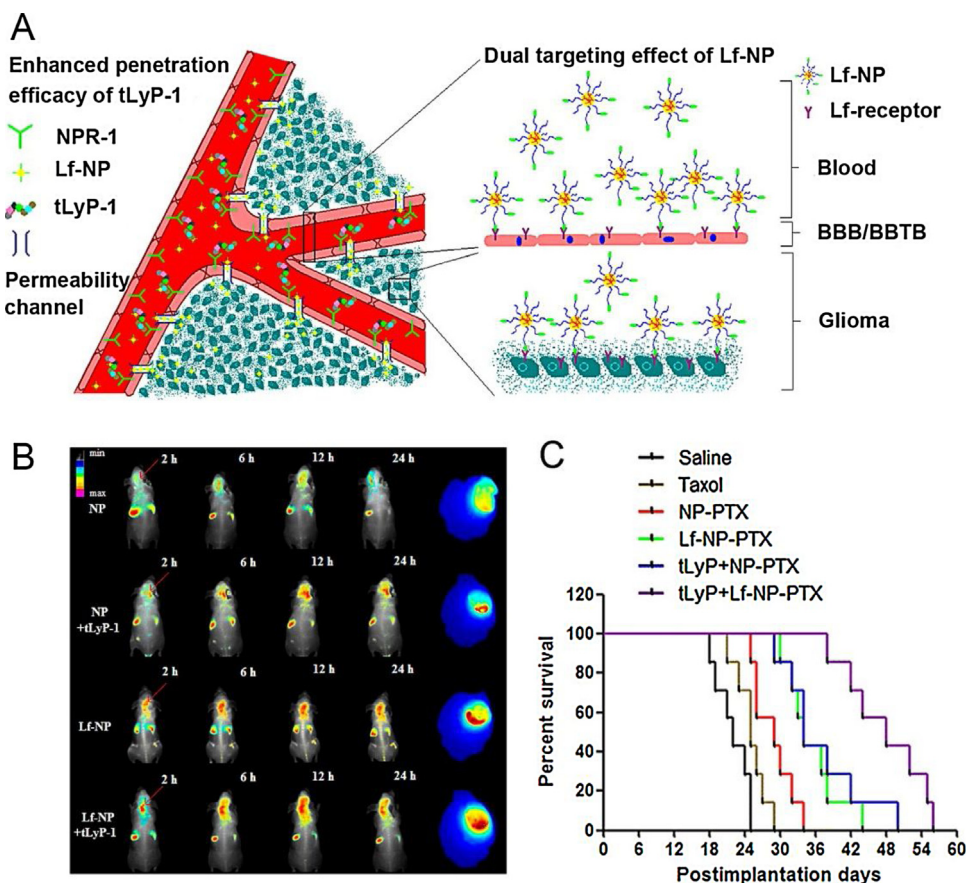


Fig. 9. (A) Schematic illustration of co-administration of lactoferrin (Lf) functionalized PEG-PLA nanoparticles with a tumor-homing peptide tLyP-1 for enhanced glioma targeting and penetration. (B) in vivo fluorescence imaging of nude mice bearing intracranial C6 glioma after intravenous injection with DiR-labeled NP, NP+tLyP-1, Lf-NP, and Lf-NP+tLyP-1. The mice were sacrificed 24 h after intravenous injection of nanoparticles with the brains collected for imaging. Red arrows: the tumor site. (C) Kaplan-Meier survival curve of mice bearing intracranial C6 glioma treated with Taxol, NP-PTX, and NP-PTX with co-administration of tLyP-1, Lf-NP-PTX, and Lf-NP-PTX with co-administration of tLyP-1 (PTX dose 5 mg/kg, tLyP-1 dose 4 μ mol/kg) and saline, respectively, every three days for two weeks ($n = 7$). Images reproduced from [52] with permission from the American Chemical Society, Copyright 2014. (For interpretation of the references to colour in this figure legend, the reader is referred to the web version of this article.)

found in cellular uptake and cytotoxicity as compared to a system without the presence of a bEnd.3 monolayer. Firstly, the cellular uptake and cytotoxicity of DTX-loaded nanoparticles in glioma cells or spheroids were significantly decreased due to the partial retention of nanoparticles by the bEnd.3 monolayer, which also explains the possible reason why this nanomedicine has poor anti-glioma efficacy in vivo. Moreover, the presence of the bEnd.3 monolayer will more accurately reflect the functions of different ligands. For example, without the bEnd.3 monolayer, AsNP had better C6 spheroid penetration ability than TNP due to receptor-mediated endocytosis. However, in the presence of a bEnd.3 monolayer, the accumulation of AsNP in C6 spheroids was lower than that of TNP because of poor BBB permeation. Combining the two ligands resulted in a significantly stronger accumulation and penetration in C6 spheroids, confirming the synergistic effect of TNG peptide and AS1411 aptamer in glioma-targeted therapy. Therefore, a suitable in vitro evaluation method is important to reveal the functions of different ligands and to provide a good basis for in vivo studies.

To further improve glioma targeting and penetration of nanomedicines, Angiopep-2 and tLyP-1 peptide were conjugated to liposomes [50]. Angiopep-2 (ANG, TFFYGGSRGKRNNFKTEEY) is a ligand that targets the low-density lipoprotein receptor-related protein (LRP) receptor, which is overexpressed in both BBB and glioblastoma cells [78]. tLyP-1 peptide (CGNKRTR) is a tumor-homing peptide which has been demonstrated to be able to mediate tissue penetration through neuropilin-1 dependent C-end Rule

internalization [109]. Moreover, vascular endothelial growth factor (VEGF) siRNA and chemotherapeutic docetaxel (DTX) were both loaded into liposomes to achieve anti-angiogenesis and apoptosis effects, respectively. The synergistic effect of Angiopep-2 and tLyP-1 was demonstrated in cellular uptake studies while evidence of the synergistic effect in vivo is lacking as single-targeting control groups were not used. In addition, a subcutaneous U87MG glioma model may not be suitable to evaluate the BBB penetration ability of these dual-ligand liposomes. In another anti-glioma study, tLyP-1 was also chosen to enhance the tumor penetration ability of nanocarriers but in a different way [52]. It was reported that tLyP-1 can trigger tumor penetration of a co-administered compound by activating the CendR pathway [109]. In Miao's study, PEG-PLA nanoparticles (NP) were modified with lactoferrin (Lf), which possesses dual-targeting ability to both BBB and glioblastoma cells, and co-administered with tLyP-1 to C6 orthotopic glioma bearing mice [52] (Fig. 9). Compared to PTX-loaded single-targeting Lf-NP, co-administration with tLyP-1 enhanced the accumulation and penetration of Lf-NP in glioma, leading to a significant prolonged survival time of glioma-bearing mice. Notably, in 3D glioma spheroids, no increase in the penetration of Lf-NP was found when tLyP-1 was co-administered, due to lack of expression of the receptor of tLyP-1, neuropilin-1 (NRP1), on the avascular tumor spheroids. However, it is reported that NRP1 receptors are overexpressed on both glioma cells and neovascular endothelial cells

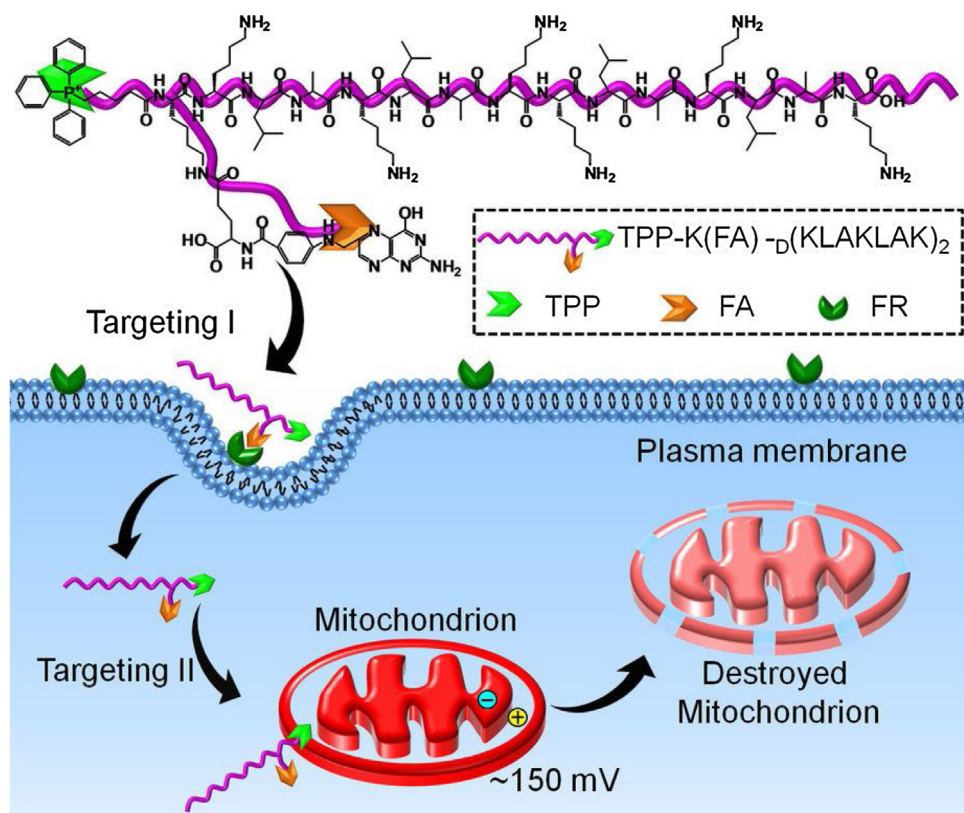


Fig. 10. Dual-targeting pro-apoptotic peptide to selectively target cancer cells and specifically damage mitochondria to initiate programmed cell death. Images reproduced from [47] with permission from Nature Publishing. Copyright 2013.

[110]. The lack of the expression of NRP1 on C6 glioma cells in this study may be due to cell line origin or culture method of the cells.

The folate receptor (FR), a 38 kDa glycosyl-phosphatidylinositol-anchored glycoprotein, is significantly upregulated on many cancer cells compared to normal tissue [6]. Folate ligands, which have high binding affinity to folate receptors, are widely used for tumor-targeted delivery. However, it is rare that the target receptor is exclusively over-expressed in target cells alone. To further improve the selectivity of nanomedicines, folic acid (FA) and mAb225 (a monoclonal antibody directed against the EGFR) were both decorated on DOX-loaded liposomes and their targeting efficiency was evaluated on FR⁺ EGFR⁺ KB cells (human epidermoid carcinoma cells) [46]. MTT assay showed that minimal viability of KB cells was achieved at 400 FA or 6 mAb225 ligands for liposomes with one ligand. Interestingly DOX-loaded dual-targeting liposomes with the optimal number of FA and mAb225 (200 FA and 3 mAb225) displayed a much higher cytotoxicity as compared to single FA or mAb225 modified liposomes with the same number of ligands as used in the dual ligand approach. That is, dual-targeting DOX-loaded liposomes with optimal number of ligands exhibited strong cytotoxicity only to cells expressing both FR and EGFR. The high selectivity was reached because the number of ligands on double ligand liposomes was suboptimal for efficient uptake of the liposomes by the cells using one receptor, while an optimal combination of ligands was reached using the two available receptors on the cells. Besides using cytostatic drugs (e.g. DOX) to directly kill tumor cells, inducing cell apoptosis is another effective approach for antitumor therapy. As is well known, mitochondria play a critical role in the cell metabolism and also serve as a control center for cell apoptosis. Mitochondrial damage will trigger cell death by signaling cascades and mitochondria-dependent apoptosis [111]. To efficiently target tumor mitochondria, an FA and triphenylphos-

phonium (TPP) containing dual-targeting pro-apoptotic peptide KLA (DTP) was developed [47]. TPP cation is a mitochondrial targeting agent, which specifically delivers the pro-apoptotic peptide to mitochondria after internalization by cancer cells (Fig. 10). In FR overexpressing KB cells (FR⁺⁺) and HeLa cells (FR⁺), DTP exhibited much higher cytotoxicity than FA-KLA, demonstrating the mitochondrial targeting effect of TPP. Notably, TPP-KLA alone displayed low cytotoxicity in the two cells due to lack of efficient uptake. In FR-negative (FR⁻) normal cell line of COS7 cells, poor cytotoxicity was found in all the formulations (KLA, FA-KLA, TPP-KLA and DTP), suggesting that efficient uptake by FR-mediated endocytosis is an indispensable primary step for mitochondrial targeting of TPP. Besides mitochondria, nuclei are also important subcellular targets, especially for DNA delivery. The major barrier for efficient gene expression mediated by polymer vectors is usually the nuclear transport step. Therefore, Zhang et al. constructed quaternary complexes poly(amidoamine) PAMAM/DNA/HMGB1/HB for efficient DNA delivery to cancer cell nuclei. HMGB1 is a nuclear protein containing two nuclear localization signals (NLSs) for nuclear transport and the biotin coupled to heparin (heparin-biotin) (HB) specifically targets biotin receptors overexpressed on the tumor cell surface. Confocal microscopy revealed that both increased cellular uptake and nuclear accumulation of DNA was found in HeLa cells treated with PAMAM/DNA/HMGB1/HB as compared with PAMAM/DNA/HMGB1 and PAMAM/DNA/HB, leading to the highest transfection efficiency.

Targeting ligand combined with cell penetrating peptides

Since the payloads of nanocarriers such as drugs and genes exert their actions intracellularly, after arrival of the nanocarriers at the tumor site, they have to pass the tumor cell membrane

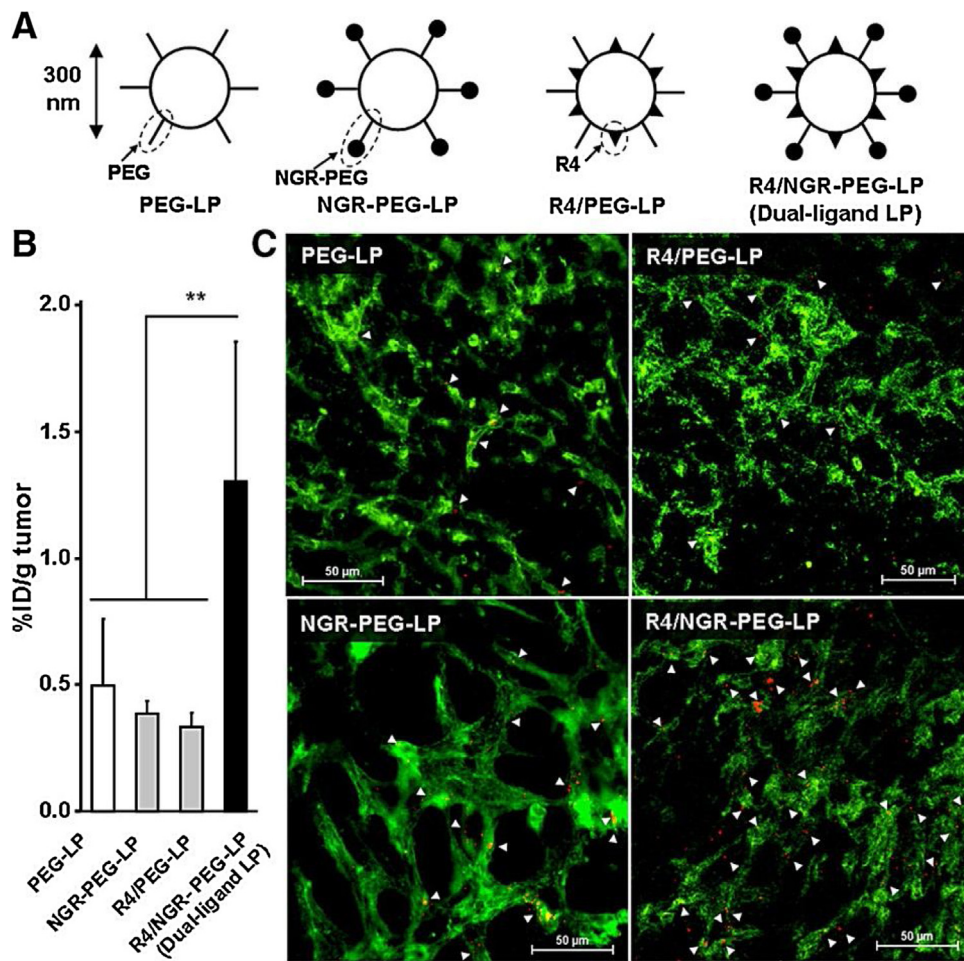


Fig. 11. Tumor accumulation and localization of dual-ligand liposomes (LP) in human renal tumor bearing mice. (A) Schematic illustration of prepared formulations. LPs were modified with either PEG, NGR modified PEG or R4. Dual-ligand LP was prepared by modification with both NGR modified PEG and R4. (B) Tumor accumulation at 24 h after systemic administration of formulations labeled with [³H] is represented by %ID/g tissue (the mean \pm SD, n=4). **P<0.01. (C) Images of unfixed tumor tissues intravenously treated with each formulation labeled with rhodamine (0.5 μ mol lipid/mouse). Tumor endothelial cells were labeled with lectin (green). Arrow heads point red signals (liposomes) along with blood vessels. Images reproduced from [61] with permission from Elsevier, Copyright 2012. (For interpretation of the references to colour in this figure legend, the reader is referred to the web version of this article.)

barrier [112]. Nanocarriers modified with one or more targeting ligands display a more rapid and efficient cellular uptake compared with non-targeted counterparts due to receptor-mediated endocytosis. However, the uptake efficacy of nanocarriers by tumor cells is still limited since the receptors on these cells dynamically change with tumor progression [10] and saturation of receptor-ligand binding will occur [56]. The discovery of cell-penetrating peptides (CPPs) shows great promise in overcoming the cell membrane barrier and significantly enhanced cellular uptake was found using CPP-functionalized nanocarriers [113–115]. However, in vivo application of nanocarriers which are only functionalized with CPPs is limited since the non-specificity of CPPs may also induce strong penetration of normal cells, leading to systemic toxicity [116,117]. Moreover, the CPP-functionalized nanocarriers may be easily recognized by the RES due to the high density of surface positive charge [118]. Therefore, the use of nanocarriers which are modified with combinations of targeting ligands and CPPs at the surface seems to be an effective way to overcome this problem.

TAT peptide (YGRKKRRQRRR), which is derived from the C-terminal end of the HIV-TAT protein, is the most widely studied CPP [119]. It has been reported that by conjugating both RGD and TAT peptide to short interfering RNA-quantum dots (siRNA-QD) conjugates, selective accumulation of QD could be established in a

mixture of $\alpha_v\beta_3$ -overexpressing U87 cells and $\alpha_v\beta_3$ -lowexpressing neuronal PC-12 cells, and also maximal internalization and gene silencing efficacy were achieved, confirming the active-targeting effect of RGD and the cell-penetrating ability of TAT [54]. Effective delivery of siRNA was also demonstrated by introducing RGD and TAT onto a PEG-(PCL-g-spermine) micellar siRNA complex [55]. Compared with single ligand DOX loaded RGD- or TAT-micelles, RGD and TAT dual ligand-functionalized micelles showed significantly enhanced cellular uptake and decreased P-gp expression in MDA435/LCC6 resistant cells, leading to greatly increased intracellular DOX accumulation and cytotoxicity. The mechanism by which TAT can greatly enhance the cellular uptake of nanocarriers is still unclear, but many studies have suggested that the electrostatic interaction between the positive residues of TAT and the negatively charged glycosaminoglycans such as heparin sulfate proteoglycans (HSPGs) on the cell surface is the necessary first step before internalization [120,121]. However, the subsequent uptake pathways for TAT-functionalized nanocarriers are diverse most probably due to variation in types of nanocarriers used, particle size, zeta potential and so on [119]. The cellular uptake mechanisms may become more complicated in targeting ligand-TAT co-functionalized nanocarriers, which may involve macropinocytosis, clathrin and caveolin-mediated

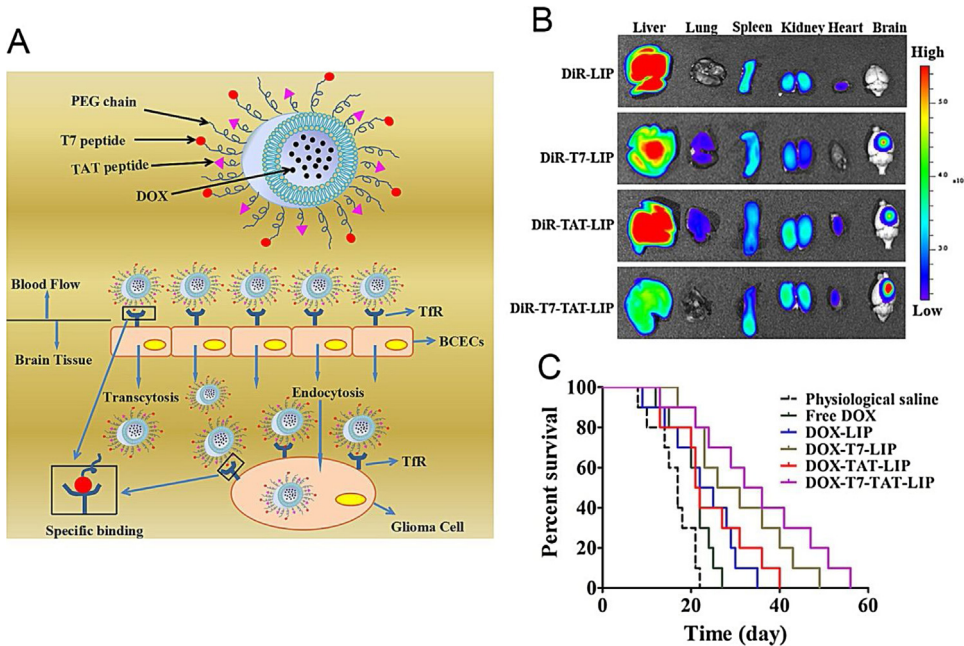


Fig. 12. (A) Schematic illustration of DOX-loaded T7 and TAT co-modified liposomes (DOX-T7-TAT-LIP). DOX-T7-TAT-LIP could specifically bind to transferrin receptors expressed on BCECs and transport across the BBB through a synergistic effect. Then the liposomes could accumulate in the glioma selectively, penetrate into the core region of the tumor, and release drugs. (B) Ex vivo images of C6 tumor-bearing BALB/c mice 4 h after injection of DiR-labeled liposomes. (C) Survival curve of the brain glioma-bearing mice treated with different formulations at a dose of 2.5 mg/kg DOX, n = 10. Images reproduced from [67] with permission from the American Chemical Society, Copyright 2014.

endocytosis [67]. However, whether introducing TAT onto active-targeting nanocarriers will produce new endocytic pathways or change the proportions of different pathways involved is still unclear since the majority of studies only focused on the uptake mechanisms of dual-ligand nanocarriers, lacking comparison with single-ligand nanocarriers. The in vitro studies have demonstrated the advantages of combining targeting ligands with CPPs [54,55,69], while more factors should be considered before application in vivo since the positively charged CPPs may result in rapid clearance of nanocarriers from blood by the RES system or non-specific penetration to normal cells. In Li's study, RGDDyC and TAT peptide were directly decorated on the surface of PAMAM through N-hydroxysulfosuccinimide-polyethylene glycol-maleimide (Sulfo-NHS-PEG-MAL) [53]. Although RGDDyC and TAT dual-ligand PAMAM showed increased tumor accumulation compared with single-ligand RGDDyC-PAMAM in MCF-7 tumor-bearing mice, substantial amounts of particles were located in the liver and spleen, probably due to the small size (~14 nm) [107] and positive charge (+3.4 mV) leading to rapid recognition by the reticuloendothelial system (RES) [122]. In order to make better use of CPPs, several strategies have been developed. Harashima's group designed dual-ligand PEGylated liposomes, in which the targeting ligand (RGD or NGR) was attached to the end of PEG and the CPP, stearylated oligoarginine (STR-RX), was coated onto the surface of the liposomes. In this way, CPPs can be shielded by a long PEG layer, while still exerting their penetration ability in the process of targeting ligand-receptor recognition, which allow CPPs to come close to the surface of the target cells. Using this strategy, selective and efficient cellular uptake was found in vitro [53,58–60]. Moreover, tumor accumulation of NGR/R4 liposomes was significantly higher than that of single-ligand NGR liposomes or R4 liposomes in OS-RC-2 renal carcinoma bearing mice (Fig. 11) [61]. Similar to this strategy, TAT was directly bound to mesoporous silica nanoparticles (MSNs) while RGD was conjugated to PEG₁₅₀₀ attached to the surface of the MSNs [57]. Enhanced cellular

uptake and nuclear targeting were both achieved by applying DOX-loaded MSNs-RGD/TAT, leading to almost complete eradication of the tumor in HeLa cervical cancer bearing mice. However, direct attachment of TAT peptide to the surface of nanocarriers may limit effective interaction of TAT with the cell surface [123]. Therefore, Heis group developed PEGylated liposomes, in which TAT was conjugated to relatively short PEG₂₀₀₀ and transferrin (TF) was attached to PEG₃₅₀₀. In comparison with TF-liposomes or TAT-liposomes, TF/TAT-liposomes showed a stronger tumor accumulation in HepG2 liver cancer bearing mice [63] or B16 melanoma bearing mice [64]. Moreover, by conjugating T7 peptide (high affinity for TfR) to PEG₂₀₀₀ and TAT peptide to PEG₁₀₀₀, DOX-loaded liposomes exhibited strong BBB permeation ability and anti-glioma efficacy in orthotopic glioma bearing mice (Fig. 12) [67]. The synergistic effect of a targeting ligand and CPPs has also been demonstrated with FA and TAT dual-ligand liposomes, in which FA was conjugated to PEG₅₀₀₀ and TAT to PEG₂₀₀₀, allowing effective shielding of TAT [70].

Another strategy to hide TAT at the surface of the nanocarrier is by the introduction of long PEG chains containing stimuli-responsive bonds [56,66,71,72]. When nanocarriers arrive at the tumor site, PEG will be removed due to cleavage of stimuli-responsive bonds, leading to exposure of TAT. Torchilin's group designed antibody mAb 2C5 and TAT co-functionalized liposomes with long PEG containing matrix metalloprotease 2 (MMP-2)-sensitive bonds [71] or pH-sensitive hydrazone bonds [72]. However, the promising results of these nanocarriers were only shown in vitro by either adding MMP-2 or by changing the pH of the medium to 5.0, which may not represent the real in vivo conditions as the concentration of enzymes and the pH in the tumor microenvironment vary in different types of tumors or in different regions of the tumor tissue [124–126]. Mei et al. developed liposomes functionalized with RGD, TAT and cleavable PEG containing reduction-sensitive disulfide bonds [56]. Twenty four hours after intravenous injection of these liposomes into HepG2-

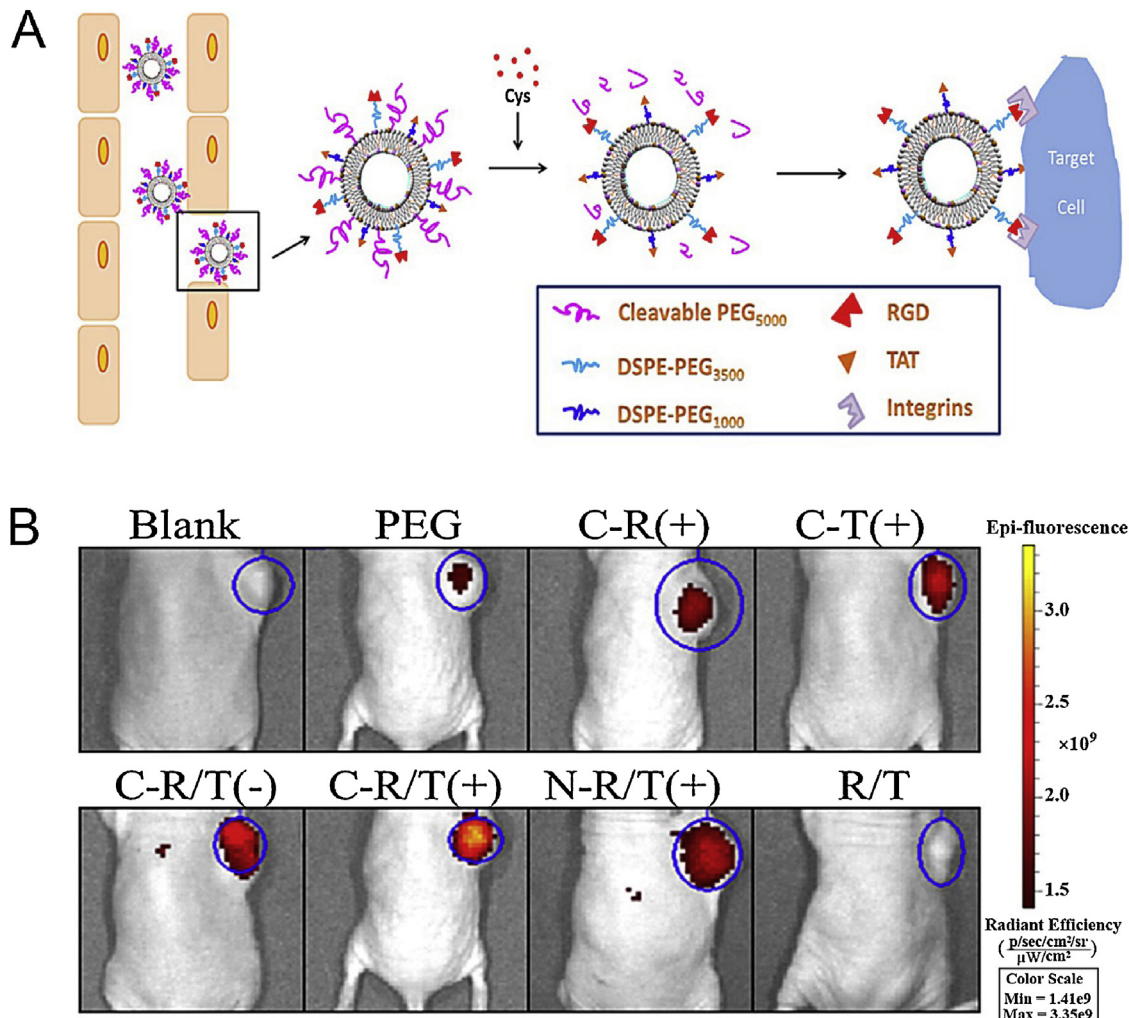


Fig. 13. (A) Schematic illustrations of multistage liposomes modified with RGD, TAT and cleavable PEG (C-R/T). (B) *in vivo* fluorescence imaging of HepG2-xenografted nude mice after injection of DIR-labeled liposomes. PEG liposome (PEG), the cleavable PEG and RGD or TAT co-modified liposome (C-R, C-T), the non-cleavable PEG, RGD and TAT co-modified liposome (N-R/T). +, – represent with or without injection of L-Cys. Images reproduced from [56] with permission from Elsevier, Copyright 2014.

xenografted nude mice, the reducing agent L-cysteine (120 mg/kg) was also intravenously injected into the mice to cleave the disulfide bonds of PEG and expose TAT, resulting in enhanced accumulation of liposomes in tumor tissue (Fig. 13).

Since CPPs are positively charged, another feasible approach is to temporarily protect CPPs with a negatively charged compound by electrostatic interaction [65,68]. Gao et al. constructed Angiopep-2 and activatable CPP (ACP) dual-functionalized nanoparticles (AnACNPs) for glioma targeted delivery (Fig. 14). CPP (R8 peptide) was conjugated to a negatively charged EEEEEE (E8) via a matrix metalloproteinase-2 (MMP-2)-sensitive linker PLGLAG. After transport across the BBB by low-density lipoprotein receptor-related protein-1 (LRP-1) mediated transcytosis, R8 peptide could be exposed by cleavage of PLGLAG by MMP-2, of which the expression level is high in the glioma site [127]. DTX loaded dual-ligand nanoparticles displayed a better distribution and deep penetration in glioma tissue compared with single Angiopep-2 nanoparticles (ACNPs) or R8 nanoparticles (CNPs), leading to significantly longer survival times of orthotopic glioma bearing mice. Han et al. prepared DOX-loaded mesoporous silica nanoparticles (MSN) with a multi-layered positive/negative/positive structure (first layer is TAT coupled to MSN, second layer is poly(allylamine) modified with citraconic anhydride (PAH-Cit) and the third layer is

galactose-modified trimethyl chitosan-cysteine (GTC) conjugate) to encapsulate vascular endothelial growth factor (VEGF) siRNA. Galactose ligands were conjugated to the GTC outer layer to facilitate the cellular uptake of the multi-layered nanocomplexes (MLNs) via galactose receptor-mediated endocytosis in human hepato-carcinoma QGY-7703 cells. After endocytosis and possible fusion of the endosomes with lysosomal compartments where the pH is decreased to 4.0–5.0, nanocomplexes undergo structural disassembly and endosomal/lysosomal escape, releasing siRNA into the cytoplasm and delivering DOX to nuclei via TAT-mediated targeting [68]. A high tumor inhibition rate (91.3%) was achieved in QGY-7703 hepato-carcinoma bearing mice using the multi-layered nanocomplexes due to efficient delivery of DOX and siRNA.

Besides conjugating CPPs to nanocarriers, encapsulation of CPPs provides an interesting method to mask CPPs. Yang et al. developed NGR-functionalized thermosensitive liposomes (TSL) containing CPP-DOX conjugates in their aqueous interior. CPPs (CKRRMK-WKK), derived from penetratin, could be activated via a heat stimulus and was used as the secondary targeting moiety to more efficiently deliver DOX to nuclei (Fig. 15) [62]. By locally heating the tumors to 42 °C for 30 min, CPP-DOX/NGR-TSL displayed the best tumor inhibition efficacy in HT-1080 human fibrosarcoma xenografts bearing nude mice. Although promising, this approach

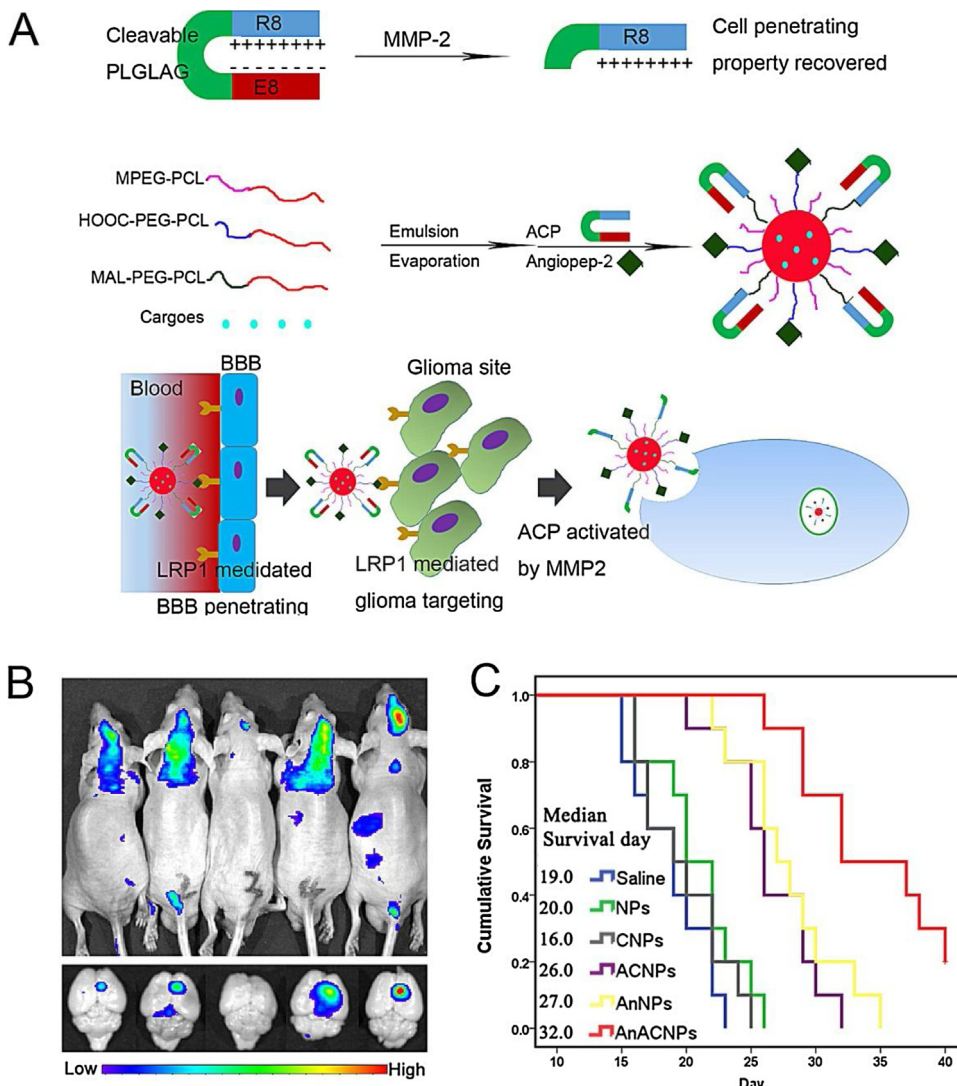


Fig. 14. (A) Illustration of the approach using Angiopep-2 and activatable cell-penetrating peptide dual-functionalized nanoparticles for glioma targeted therapy. The cell penetrating property could be activated by MMP-2. AnACNPs could transport through the BBB and target to glioma because of angiopep-2 could bind with LRP1 that is expressed on BBB and glioma cells. ACP could be activated in the glioma site owing to the high expression level of MMP-2, which led to improved cell penetrating property. (B) *In vivo* imaging of whole body and *ex vivo* imaging of brain from mice treated with different DiR-loaded formulations. (C) Survival curve of the brain glioma bearing mice treated with saline, docetaxel loaded NPs, CNPs, ACNPs, AnNPs or AnACNPs. $n = 10$. Images reproduced from [65] with permission from the American Chemical Society. Copyright 2014.

requiring an external stimulus seems only feasible if the tumor can be locally heated without damaging the surrounding tissue.

The various strategies introduced above combining targeting ligands and CPPs in ingenious ways, resulted in synergistic effects of targeting ligands and CPPs both in vitro and in vivo. It was noticed that besides enhanced cellular uptake, also improved tumor accumulation and penetration were observed in various studies using targeting ligand-CPP dually functionalized nanocarriers [53,56,57,61,63–65,67]. Deep tumor penetration of nanocarriers is difficult to achieve due to the elevated interstitial fluid pressure (IFP) [128] and dense extracellular matrix (ECM) [129] of tumor tissue, leading to limited antitumor efficacy of nanomedicines. The mechanisms of better tumor penetration achieved by targeting ligand-CPP nanocarriers are still unclear and need to be further studied. One possible reason may be that efficient cellular uptake creates higher diffusion gradients which enhance the direct transport of nanocarriers into the tumor [7]. If nanocarriers can't be taken up efficiently, they will accumulate near leaky blood vessels after

extravasation. This roadblock effect could hinder the subsequent accumulation of the carriers at the tumor site [130]. In addition, IFP and ECM will dynamically change with tumor progression. It has been reported that in glioma the ECM will be degraded by highly-expressed matrix metalloproteinases (MMPs), which is required for glioma invasion [127]. The decreased density of ECM in time helps to enhance the tumor penetration of nanocarriers especially for those nanocarriers, which are efficiently taken up by cells.

Besides CPPs, another peptide, iRGD, which contains an RGD motif with a protease site and a cryptic Cend Rule (CendR) motif (R/KXXR/K), shows tumor homing ability *via* binding to $\alpha_v\beta_3/\beta_5$ integrins. Followed by a proteolytic cleavage, the CendR motif is exposed that binds to NRP-1 and triggers tissue penetration [131]. Sha et al. constructed recombinant protein anti-EGFR-iRGD that could target both the EGFR extracellular domain and the integrin $\alpha_v\beta_3/\beta_5$. It was found that this protein spread extensively throughout both human gastric adenocarcinoma BGC-823 cell spheroids and also through the BGC-823 tumor mass [132].

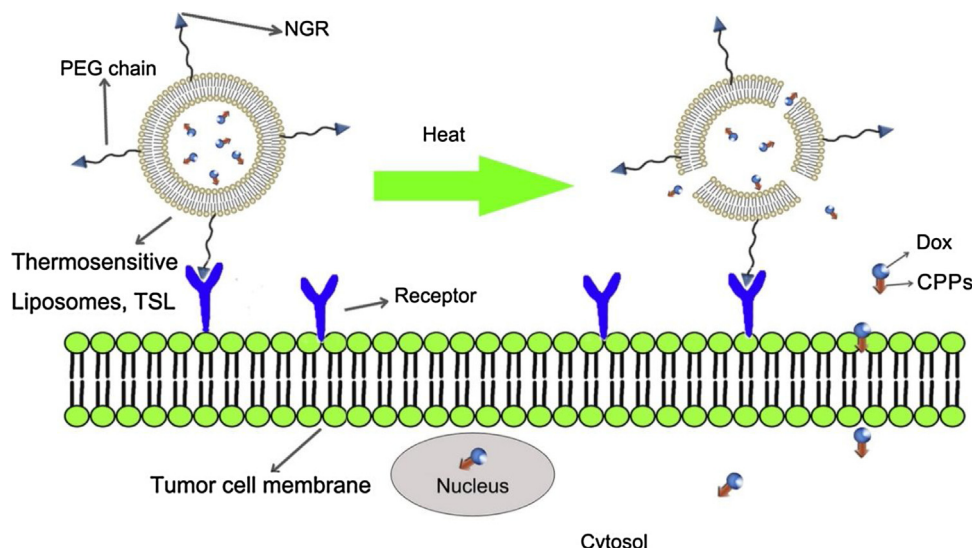


Fig. 15. Proposed schematic diagram of NGR-targeted TSL containing CPP-Dox conjugates for drug delivery to cancer cells under heat-stimulation. Images reproduced from [62] with permission from Elsevier, Copyright 2014.

In addition, with the combined use of PTX and EGFR-iRGD a better tumor inhibition effect was witnessed as compared to the clinically-used antibody cetuximab plus PTX in BGC-823 tumor-bearing mice [133]. Interestingly, the co-administration of iRGD with nanomedicines was also effective in facilitating tumor penetration of the nanomedicine [134–136]. Co-administration of iRGD with PTX-loaded MT1-AF7p peptide modified PEG-PLA nanoparticles significantly prolonged the survival time of C6 orthotopic glioma bearing mice, probably due to enhanced tumor penetration by iRGD and the active-targeting effect of MT1-AF7p to membrane type-1 matrix metalloproteinase (MT1-MMP) overexpressed on angiogenic blood vessels and glioma cells [137].

Dual-targeting with one ligand

In general, expression of one type of receptor on a particular type of cell allows targeting of nanosystems using the corresponding ligand. However, in some tumor microenvironments, one type of receptor is overexpressed on two kinds of cells and one specific ligand can be used to target both types of cells (dual targeting). The most frequently used dual-targeting approach with one ligand is to target both neovascular cells and tumor cells. As is well known, angiogenesis is required for invasive tumor growth and metastasis and constitutes an important factor in the control of cancer progression [138]. Targeting and inhibiting both neovascular cells and tumor cells, which overexpress the same receptor, with drug laden nanosystems decorated with the appropriate ligand may result in more effective tumor treatment, than using systems with a ligand for one type of cell. The most attractive receptors overexpressed on both neovascular cells and tumor cells are integrins, which play an important role in cell-cell and cell-matrix interactions [96]. RGD peptide has a high affinity to $\alpha_v\beta_3$ integrins, making it a good candidate for dual-targeting both neovascular cells and tumor cells. Zhu et al. developed RGD functionalized PEG-PAMAM-cis-aconityl-doxorubicin (PPCD) conjugate and the dual-targeting effect was studied both in vitro and in vivo [73]. Compared with non-targeted DOX-loaded PPCD, DOX-loaded RGD-PPCD showed a 1.46-fold increase in uptake in B16 melanoma probably due to efficient uptake of RGD-PPCD by both HUVECs and B16 cells, leading to more effective inhibition of tumor growth. The dual-targeting effect of DOX-loaded RGD-PPCD was confirmed by measuring the immunofluorescence of B16

melanoma tumor sections after treatment with RGD-PPCD, which showed both apoptosis of neovascular cells as well as tumor cells. Another integrin-binding peptide which has been used in phase II trials for cancer therapy is ATN-161 (N-acetyl-proline-histidine-serine-cysteine-asparagine-amide, Ac-PHSCN-NH₂). ATN-161 has a high affinity for $\alpha_5\beta_1$ integrin, which plays a significant role in tumor angiogenesis [74]. To achieve both targeting to tumor angiogenesis and tumor cells, Ac-PHSCNK-NH₂, an ATN-161 derivative, was conjugated to DOX-loaded liposomes [74]. Higher cellular uptake and cytotoxicity were observed in both $\alpha_5\beta_1$ overexpressing HUVECs and MDA-MB-231 breast tumor cells in comparison with non-targeted DOX-liposomes, demonstrating that slightly modified ATN-161 without destroying its core sequence still possesses high integrin-binding ability. A similar efficacy in both HUVECs and MDA-MB-231 breast tumor cells was found when using tLyp-1 peptide-decorated DOX-loaded hollow mesoporous silica nanoparticles (tHMSN) [75]. tLyp-1 peptide that has been obtained by screening a phage display library has high affinity for neuropilin (NRP), which is a modular transmembrane protein and a receptor for vascular endothelial growth factor (VEGF). NRP is also highly overexpressed on the surface of both mammary cancer cells and tumor vessels. Angiogenesis also plays an important role in glioma growth and invasiveness. It has been reported that tissue factor (TF) is overexpressed on both neovascular cells and glioma cells. EGFP-EGF1 (ENP), a fusion protein derived from factor VII with special affinity for TF, was used as a carrier for PTX and this system was applied for glioma therapy [76]. PTX-loaded ENP (ENP-PTX) significantly prolonged the median survival time of orthotopic glioma-bearing mice due to the dual-targeting of neovascular cells and glioma cells in gliomas.

In breast cancer therapy, breast cancer stem cells (BCSCs), which are resistant to conventional chemotherapy and radiotherapy, are responsible for the resistance and relapse of breast cancer [95]. Since CD44 is highly expressed on both BCSCs (characterized by the CD44⁺/CD24⁻ phenotype) and breast tumor cells, nanomedicines functionalized with HA, which specifically binds to CD44, may be a promising tool to treat breast cancer. Goodarzi et al. showed that HA-DTX conjugates could be efficiently internalized into both MDA-MB-231 breast tumor cells and MCF-7 cancer stem-like cells due to CD44-mediated endocytosis, leading to high cytotoxicity in both cells [94]. It has been reported that the use of a combination of conventional chemotherapy drugs and anti-CSCs

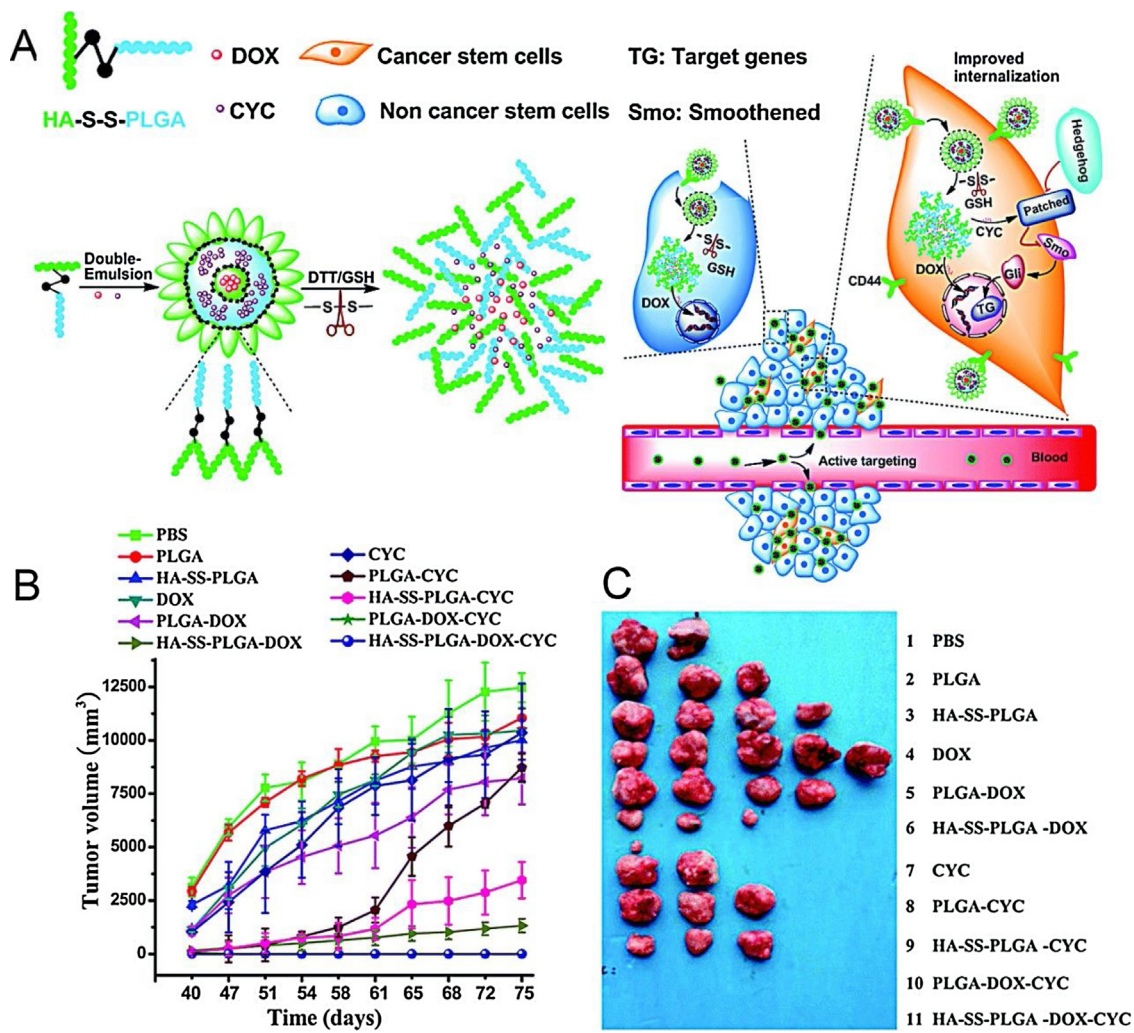


Fig. 16. (A) The preparation and possible antitumor mechanism of dual-drug (DOX and CYC) loaded HA-SS-PLGA nanoparticles. (B) Tumor volume curve after discontinuing the treatment at day 40 in an orthotopic mammary fat pad MDA-MB-231 tumor growth model. Data are expressed as the mean \pm SD ($n=5$). (C) Photos of excised tumors at day 75. Images reproduced from [95] with permission from the Royal Society of Chemistry, Copyright 2015.

drugs is a promising strategy for efficient inhibition of cancer. Hu et al. constructed hyaluronic acid-cystamine-poly(lactic-co-glycolic acid) (HA-SS-PLGA) to deliver DOX and cyclopamine (CYC, a primary inhibitor of the hedgehog signaling pathway of CSCs) to a CD44-overexpressing MDA-MB-231 breast CSC subpopulation and bulk breast cancer cells (Fig. 16) [95]. Importantly, HA-SS-PLGA-DOX-CYC displayed complete inhibition of the tumor growth in an orthotopic mammary fat pad MDA-MB-231 tumor growth model, while the tumor of mice treated with HA-SS-PLGA-DOX or HA-SS-PLGA-CYC still rapidly proliferated after withdrawal of the treatment, indicating that efficient killing of both CSCs and tumor cells plays an important role in inhibiting tumor growth.

Glioma differs from other tumors because of the presence of the BBB. Therefore, ligands possessing both BBB and glioma cell targeting ability show great promise in glioma targeted delivery and therapy. Low density lipoprotein (LDL) receptor related protein (LRP), a member of the LDL receptor (LDLR) family, is overexpressed on both BBB and glioblastoma cells. Several distinct ligands such as angiopep-2 [77–81], apoE [83,84], lactoferrin [85–89], transferrin [90–93] and a peptide that is obtained by phage display screening (peptide 22) [82] have high affinity for LRP. Nanocarriers functionalized with these ligands showed enhanced glioma imaging and/or inhibition effects compared with non-targeted counterparts. Among these ligands, angiopep-2 attracts more attention as

this small peptide is easier to conjugate to nanosystems for instance via the thiol-maleimide reaction [78,80] than proteins while still presenting a high BBB and tumor cell targeting ability. Moreover, using peptides may be more attractive than using antibodies when combinations with other ligands are projected since they create less steric hindrance.

Conclusions

Based on the types and levels of receptors that are overexpressed on tumor cells and other cells in the specific tumor microenvironment, various dual-ligand nanomedicines have been designed to gain superior cell selectivity, cellular uptake or tumor penetration ability, showing great advantages in tumor targeted therapy. From the studies above, several aspects should be taken into consideration when designing dual-ligand nanomedicines. Firstly, ligand density, position, affinity with receptors and activity after conjugation have a great impact on the targeting effect. These factors can be evaluated and optimized via *in vitro* studies, providing a reliable basis for *in vivo* application. Therefore, determination of receptor expression on cells and properly designed *in vitro* studies are very important. Secondly, when applied *in vivo*, the first important factor is the stability of the nanomedicine, which is a prerequisite to allow the ligands to exert their function at the tumor site. Various

factors can affect the stability of nanomedicines such as the critical micelle concentration, stimulus-sensitive crosslinking and the balance between PEGylation and ligand modification (shielding). However, although well designed, good targeting efficacy of dual-ligand nanomedicines *in vitro* may not necessarily lead to optimal results *in vivo* due to the complicated tumor microenvironment (e.g. dynamically changing expression levels of receptors and competitive binding to receptors from endogenous ligands). Therefore, more efforts should be undertaken to effectively monitor the *in vivo* tumor microenvironment, allowing optimization of the targeting effect of dual-ligand nanomedicines. In addition, the underlying mechanisms of the synergistic effect of dual-ligand nanomedicines should also be carefully investigated (such as ligand-receptor binding rate and sequence, and subsequent uptake pathways) to provide a solid basis for their advantages over simple mixtures of single ligand nanomedicines. Furthermore, although dual-targeted nanomedicines show promising results in cancer therapy, we should realize that their clinical translation is still a formidable challenge. Until now, none of the ligand-targeted nanomedicines have been approved probably due to two major aspects: ambiguous active-targeting effect in heterogeneous human tumors and the difficulties encountered in large-scale and reproducible production while maintaining the activity of targeting ligands. Therefore, future studies should focus more on human tumor biology (e.g. by establishing models that are more close to human tumors). Besides, more attention should be paid to the design, production and control aspects of dual-targeted nanomedicines to facilitate possible clinical translation.

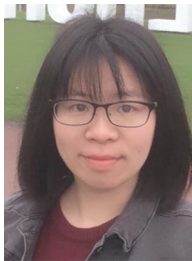
Acknowledgement

This work is financially supported by the National Natural Science Foundation of China (NSFC 51633005).

References

- [1] X. Wang, L. Yang, Z.G. Chen, D.M. Shin, CA Cancer J. Clin. 58 (2008) 97–110.
- [2] A. Wicki, D. Witzigmann, V. Balasubramanian, J. Huwyler, J. Controlled Release 200 (2015) 138–157.
- [3] F. Danhier, O. Feron, V. Préat, J. Controlled Release 148 (2010) 135–146.
- [4] F. Danhier, J. Controlled Release 244 (2016) 108–121.
- [5] J.W. Nichols, Y.H. Bae, J. Controlled Release 190 (2014) 451–464.
- [6] J.D. Byrne, T. Betancourt, L. Brannon-Peppas, Adv. Drug Deliv. Rev. 60 (2008) 1615–1626.
- [7] M. Wang, M. Thanou, Pharmacol. Res. 62 (2010) 90–99.
- [8] R. van der Meel, L.J. Vehmeijer, R.J. Kok, G. Storm, E.V. van Gaal, Adv. Drug Deliv. Rev. 65 (2013) 1284–1298.
- [9] S.C. Tang, P. Kumthekar, A.J. Brenner, S. Kesari, D. Piccioni, C.K. Anders, et al., Ann. Oncol. 27 (2016) 3240.
- [10] G. Di Lorenzo, G. Tortora, F.P. D'Armiento, G. De Rosa, S. Staibano, R. Autorino, et al., Clin. Cancer Res. 8 (2002) 3438.
- [11] N. Platet, A.M. Cathiard, M. Gleizes, M. Garcia, Crit. Rev. Oncol. Hematol. 51 (2004) 55–67.
- [12] J.A. Koenig, J.M. Edwardson, Trends Pharmacol. Sci. 18 (1997) 276–287.
- [13] F. Morgillo, H.Y. Lee, Drug Resist. Updat. 8 (2005) 298–310.
- [14] H.E. Jones, J.M.W. Gee, I.R. Hutcheson, J.M. Knowlden, D. Barrow, R.I. Nicholson, Endocr-Relat. Cancer 13 (2006) S45–S51.
- [15] A. Sartore-Bianchi, L. Trusolino, C. Martino, K. Bencardino, S. Lonardi, F. Bergamo, et al., Lancet Oncol. 17 (2016) 738–746.
- [16] S.M. Leto, F. Sassi, I. Catalano, V. Torri, G. Migliardi, E.R. Zanella, et al., Clin. Cancer Res. 21 (2015) 5519–5531.
- [17] J. Baselga, I. Bradbury, H. Eidtmann, S. Di Cosimo, E. de Azambuja, C. Aura, et al., Lancet 379 (2012) 633–640.
- [18] R.E. Kontermann, MAbs 4 (2012) 182–197.
- [19] C. Huang, Z. Tang, Y. Zhou, X. Zhou, Y. Jin, D. Li, et al., Int. J. Pharm. 429 (2012) 113–122.
- [20] Y.J. Lu, K.C. Wei, C.C. Ma, S.Y. Yang, J.P. Chen, Colloids Surf. B Biointerfaces 89 (2012) 1–9.
- [21] W. Zhang, Z.L. Yu, M. Wu, J.G. Ren, H.F. Xia, G.L. Sa, et al., ACS Nano 11 (2017) 277–290.
- [22] J.H. Fang, Y.H. Lai, T.L. Chiu, Y.Y. Chen, S.H. Hu, S.Y. Chen, Adv. Healthc. Mater. 3 (2014) 1250–1260.
- [23] H. Wang, S. Zhang, Z. Liao, C. Wang, Y. Liu, S. Feng, et al., Biomaterials 31 (2010) 6589–6596.
- [24] H.W. Child, P.A. del Pino, J.M. De La Fuente, A.S. Hursthouse, D. Stirling, M. Mullen, et al., ACS Nano 5 (2011) 7910–7919.
- [25] E. Kluza, D.W. van der Schaft, P.A. Hautvast, W.J. Mulder, K.H. Mayo, A.W. Griffioen, et al., Nano Lett. 10 (2010) 52–58.
- [26] E. Kluza, I. Jacobs, S.J. Hectors, K.H. Mayo, A.W. Griffioen, G.J. Strijkers, et al., J. Controlled Release 158 (2012) 207–214.
- [27] Y. Nie, D. Schaffert, W. Rodl, M. Ogris, E. Wagner, M. Gunther, J. Controlled Release 152 (2011) 127–134.
- [28] Q. Xu, Y. Liu, S. Su, W. Li, C. Chen, Y. Wu, Biomaterials 33 (2012) 1627–1639.
- [29] H. Gao, Y. Xiong, S. Zhang, Z. Yang, S. Cao, X. Jiang, Mol. Pharm. 11 (2014) 1042–1052.
- [30] H. Gao, Z. Yang, S. Cao, Y. Xiong, S. Zhang, Z. Pang, et al., Biomaterials 35 (2014) 2374–2382.
- [31] C. Rangger, A. Helbok, J. Sosabowski, C. Kremser, G. Koehler, R. Prassl, et al., Int. J. Nanomed. 8 (2013) 4659–4671.
- [32] K. Han, Y. Liu, W.N. Yin, S.B. Wang, Q. Xu, R.X. Zhuo, et al., Adv. Healthc. Mater. 3 (2014) 1765–1768.
- [33] C. Shu, R. Li, Y. Yin, D. Yin, Y. Gu, L. Ding, et al., Chem. Commun. 50 (2014) 15423–15426.
- [34] D. Chen, B. Li, S. Cai, P. Wang, S. Peng, Y. Sheng, et al., Biomaterials 100 (2016) 1–16.
- [35] Y. Liu, J. Sun, W. Cao, J. Yang, H. Lian, X. Li, et al., Int. J. Pharm. 421 (2011) 160–169.
- [36] Y. Liu, J. Sun, H. Lian, W. Cao, Y. Wang, Z. He, J. Pharm. Sci. 103 (2014) 1538–1547.
- [37] G.X. Liu, G.Q. Fang, W. Xu, Int. J. Mol. Sci. 15 (2014) 15287–15303.
- [38] S. Shi, M. Zhou, X. Li, M. Hu, C. Li, M. Li, et al., J. Controlled Release 235 (2016) 1–13.
- [39] J. Chen, J. Ouyang, Q. Chen, C. Deng, F. Meng, J. Zhang, et al., ACS Appl. Mater. Interfaces 9 (2017) 24140–24147.
- [40] B. Zhang, Y. Zhang, D. Yu, Oncol. Rep. 37 (2017) 937–944.
- [41] S. Kakimoto, T. Moriyama, T. Tanabe, S. Shinkai, T. Nagasaki, J. Controlled Release 120 (2007) 242–249.
- [42] R.R. Sawant, A.M. Jhaveri, A. Koshkaryev, F. Qureshi, V.P. Torchilin, J. Drug Target. 21 (2013) 630–638.
- [43] J.Q. Gao, Q. Lv, L.M. Li, X.J. Tang, F.Z. Li, Y.L. Hu, et al., Biomaterials 34 (2013) 5628–5639.
- [44] T. Jia, Z. Sun, Y. Lu, J. Gao, H. Zou, F. Xie, et al., Int. J. Nanomed. 11 (2016) 3765–3775.
- [45] M.C. Lo Giudice, F. Meder, E. Polo, S.S. Thomas, K. Alnahdi, S. Lara, et al., Nanoscale 8 (2016) 16969–16975.
- [46] J.M. Saul, A.V. Annapragada, R.V. Bellamkonda, J. Controlled Release 114 (2006) 277–287.
- [47] W.H. Chen, X.D. Xu, G.F. Luo, H.Z. Jia, Q. Lei, S.X. Cheng, et al., Sci. Rep. 3 (2013) 3468.
- [48] H. Gao, J. Qian, S. Cao, Z. Yang, Z. Pang, S. Pan, et al., Biomaterials 33 (2012) 5115–5123.
- [49] H. Gao, Z. Yang, S. Zhang, Z. Pang, Q. Liu, X. Jiang, Acta Biomater. 10 (2014) 858–867.
- [50] Z.Z. Yang, J.Q. Li, Z.Z. Wang, D.W. Dong, X.R. Qi, Biomaterials 35 (2014) 5226–5239.
- [51] Q. Zhang, F. Li, R.-X. Zhuo, X.-Z. Zhang, S.-X. Cheng, J. Mater. Chem. 21 (2011) 4636.
- [52] D. Miao, M. Jiang, Z. Liu, G. Gu, Q. Hu, T. Kang, et al., Mol. Pharm. 11 (2014) 90–101.
- [53] J. Li, X. Zhang, M. Wang, X. Li, H. Mu, A. Wang, et al., Int. J. Pharm. 501 (2016) 112–123.
- [54] J. Jung, A. Solanki, K.A. Memoli, K. Kamei, H. Kim, M.A. Drahl, et al., Angew. Chem. Int. Edit. 49 (2010) 103–107.
- [55] X.B. Xiong, H. Uludag, A. Lavasanifar, Biomaterials 31 (2010) 5886–5893.
- [56] L. Mei, L. Fu, K. Shi, Q. Zhang, Y. Liu, J. Tang, et al., Int. J. Pharm. 468 (2014) 26–38.
- [57] L. Pan, J. Liu, Q. He, J. Shi, Adv. Mater. 26 (2014) 6742–6748.
- [58] G. Kibria, H. Hatakeyama, N. Ohga, K. Hida, H. Harashima, J. Controlled Release 153 (2011) 141–148.
- [59] J.X. Chen, H.Y. Wang, C.Y. Quan, X.D. Xu, X.Z. Zhang, R.X. Zhuo, Org. Biomol. Chem. 8 (2010) 3142–3148.
- [60] K. Takara, H. Hatakeyama, N. Ohga, K. Hida, H. Harashima, Int. J. Pharm. 396 (2010) 143–148.
- [61] K. Takara, H. Hatakeyama, G. Kibria, N. Ohga, K. Hida, H. Harashima, J. Controlled Release 162 (2012) 225–232.
- [62] Y. Yang, Y. Yang, X. Xie, X. Cai, H. Zhang, W. Gong, et al., Biomaterials 35 (2014) 4368–4381.
- [63] J. Tang, L. Zhang, Y. Liu, Q. Zhang, Y. Qin, Y. Yin, et al., Int. J. Pharm. 454 (2013) 31–40.
- [64] M. Yuan, Y. Qiu, L. Zhang, H. Gao, Q. He, Drug Deliv. 23 (2016) 1171–1183.
- [65] H. Gao, S. Zhang, S. Cao, Z. Yang, Z. Pang, X. Jiang, Mol. Pharm. 11 (2014) 2755–2763.
- [66] P. Ringhieri, C. Diaferia, S. Galdiero, R. Palumbo, G. Morelli, A. Accardo, J. Pept. Sci. 21 (2015) 415–425.
- [67] T. Zong, L. Mei, H. Gao, W. Cai, P. Zhu, K. Shi, et al., Mol. Pharm. 11 (2014) 2346–2357.
- [68] L. Han, C. Tang, C. Yin, Biomaterials 60 (2015) 42–52.
- [69] Y. Yamada, R. Furukawa, H. Harashima, J. Pharm. Sci. 105 (2016) 1705–1713.
- [70] Y. Zhu, L. Cheng, L. Cheng, F. Huang, Q. Hu, L. Li, et al., Pharm. Res. 31 (2014) 3289–3303.

- [71] L. Zhu, P. Kate, V.P. Torchilin, *ACS Nano* 6 (2012) 3491–3498.
- [72] E. Koren, A. Apte, A. Jani, V.P. Torchilin, *J. Controlled Release* 160 (2012) 264–273.
- [73] S. Zhu, L. Qian, M. Hong, L. Zhang, Y. Pei, Y. Jiang, *Adv. Mater.* 23 (2011) H84–H89.
- [74] W. Dai, T. Yang, X. Wang, J. Wang, X. Zhang, Q. Zhang, *J. Drug Target.* 18 (2010) 254–263.
- [75] Y. Liu, Q. Chen, M. Xu, G. Guan, W. Hu, Y. Liang, et al., *Int. J. Nanomed.* 10 (2015) 1855–1867.
- [76] B. Zhang, H. Wang, Z. Liao, Y. Wang, Y. Hu, J. Yang, et al., *Biomaterials* 35 (2014) 4133–4145.
- [77] D. Ni, J. Zhang, W. Bu, H. Xing, F. Han, Q. Xiao, et al., *ACS Nano* 8 (2014) 1231–1242.
- [78] H. Xin, X. Sha, X. Jiang, W. Zhang, L. Chen, X. Fang, *Biomaterials* 33 (2012) 8167–8176.
- [79] X. Sun, Z. Pang, H. Ye, B. Qiu, L. Guo, J. Li, et al., *Biomaterials* 33 (2012) 916–924.
- [80] J. Ren, S. Shen, D. Wang, Z. Xi, L. Guo, Z. Pang, et al., *Biomaterials* 33 (2012) 3324–3333.
- [81] S. Huang, J. Li, L. Han, S. Liu, H. Ma, R. Huang, et al., *Biomaterials* 32 (2011) 6832–6838.
- [82] B. Zhang, X. Sun, H. Mei, Y. Wang, Z. Liao, J. Chen, et al., *Biomaterials* 34 (2013) 9171–9182.
- [83] M. Ghosh, R.O. Ryan, *Nanomedicine* 9 (2014) 763–771.
- [84] N. Malekloou, A. Allameh, B. Kazemi, *J. Drug Target.* 24 (2016) 348–358.
- [85] H. Chen, Y. Qin, Q. Zhang, W. Jiang, L. Tang, J. Liu, et al., *Eur. J. Pharm. Sci.* 44 (2011) 164–173.
- [86] Z. Pang, L. Feng, R. Hua, J. Chen, H. Gao, S. Pan, et al., *Mol. Pharm.* 7 (2010) 1995–2005.
- [87] L. Jiang, Q. Zhou, K. Mu, H. Xie, Y. Zhu, W. Zhu, et al., *Biomaterials* 34 (2013) 7418–7428.
- [88] H. Xie, Y. Zhu, W. Jiang, Q. Zhou, H. Yang, N. Gu, et al., *Biomaterials* 32 (2011) 495–502.
- [89] Z. Su, L. Xing, Y. Chen, Y. Xu, F. Yang, C. Zhang, et al., *Mol. Pharm.* 11 (2014) 1823–1834.
- [90] W. Guo, A. Li, Z. Jia, Y. Yuan, H. Dai, H. Li, *Eur. J. Pharmacol.* 718 (2013) 41–47.
- [91] P. Zhang, L. Hu, Q. Yin, Z. Zhang, L. Feng, Y. Li, *J. Controlled Release* 159 (2012) 429–434.
- [92] Y. Cui, Q. Xu, P.K. Chow, D. Wang, C.H. Wang, *Biomaterials* 34 (2013) 8511–8520.
- [93] G. Liu, H. Shen, J. Mao, L. Zhang, Z. Jiang, T. Sun, et al., *ACS Appl. Mater. Interfaces* 5 (2013) 6909–6914.
- [94] N. Goodarzi, M.H. Ghahremani, M. Amini, F. Atyabi, S.N. Ostad, N. Shabani Ravari, et al., *Chem. Biol. Drug Des.* 83 (2014) 741–752.
- [95] K. Hu, H. Zhou, Y. Liu, Z. Liu, J. Liu, J. Tang, et al., *Nanoscale* 7 (2015) 8607–8618.
- [96] J.D. Hood, D.A. Cheresh, *Nat. Rev. Cancer* 2 (2002) 91–100.
- [97] Y. Zhu, J. Zhang, F. Meng, C. Deng, R. Cheng, J. Feijen, et al., *J. Controlled Release* 233 (2016) 29–38.
- [98] P. Zhong, H. Meng, J. Qiu, J. Zhang, H. Sun, R. Cheng, et al., *J. Controlled Release* (2016).
- [99] Y. Fang, Y. Jiang, Y. Zou, F. Meng, J. Zhang, C. Deng, et al., *Acta Biomater.* 50 (2017) 396–406.
- [100] C. Zhan, B. Gu, C. Xie, J. Li, Y. Liu, W. Lu, *J. Controlled Release* 143 (2010) 136–142.
- [101] K. Laginha, D. Mumbengegwi, T. Allen, *Biochim. Biophys. Acta* 1711 (2005) 25–32.
- [102] Y. Zhong, K. Goltsche, L. Cheng, F. Xie, F. Meng, C. Deng, et al., *Biomaterials* 84 (2016) 250–261.
- [103] Y. Zhu, X. Wang, J. Chen, J. Zhang, F. Meng, C. Deng, et al., *J. Controlled Release* 244 (2016) 229–239.
- [104] Y. Zhong, J. Zhang, R. Cheng, C. Deng, F. Meng, F. Xie, et al., *J. Controlled Release* 205 (2015) 144–154.
- [105] K.Y. Choi, H. Chung, K.H. Min, H.Y. Yoon, K. Kim, J.H. Park, et al., *Biomaterials* 31 (2010) 106–114.
- [106] E.J. Oh, K. Park, K.S. Kim, J. Kim, J.A. Yang, J.H. Kong, et al., *J. Controlled Release* 141 (2010) 2–12.
- [107] B. Wang, X. He, Z. Zhang, Y. Zhao, W. Feng, *Acc. Chem. Res.* 46 (2013) 761–769.
- [108] B. Oller-Salvia, M. Sanchez-Navarro, E. Giralt, M. Teixido, *Chem. Soc. Rev.* 45 (2016) 4690–4707.
- [109] L. Roth, L. Agemy, V.R. Kotamraju, G. Braun, T. Teesalu, K.N. Sugahara, et al., *Oncogene* 31 (2012) 3754–3763.
- [110] Q. Hu, X. Gao, G. Gu, T. Kang, Y. Tu, Z. Liu, et al., *Biomaterials* 34 (2013) 5640–5650.
- [111] J. Lopez, S.W. Tait, *Br. J. Cancer* 112 (2015) 957–962.
- [112] E. Blanco, H. Shen, M. Ferrari, *Nat. Biotechnol.* 33 (2015) 941–951.
- [113] L. Pan, J. Liu, Q. He, L. Wang, J. Shi, *Biomaterials* 34 (2013) 2719–2730.
- [114] R.E. Vandebroucke, S.C. De Smedt, J. Demeester, N.N. Sanders, *Biochim. Biophys. Acta Biomembr.* 2007 (1768) 571–579.
- [115] H. Li, T.Y. Tsui, W. Ma, *Int. J. Mol. Sci.* 16 (2015) 19518–19536.
- [116] Y. Huang, Y. Jiang, H. Wang, J. Wang, M.C. Shin, Y. Byun, et al., *Adv. Drug Deliv. Rev.* 65 (2013) 1299–1315.
- [117] H. Gao, Q. Zhang, Z. Yu, Q. He, *Curr. Pharm. Biotechnol.* 15 (2014) 210–219.
- [118] F. Alexis, E. Pridgen, L.K. Molnar, O.C. Farokhzad, *Mol. Pharm.* 5 (2008) 505–515.
- [119] V.P. Torchilin, *Adv. Drug Deliv. Rev.* 60 (2008) 548–558.
- [120] R. Pan, W. Xu, Y. Ding, S. Lu, P. Chen, *Mol. Pharm.* 13 (2016) 1366–1374.
- [121] C. Urbinati, S. Nicoli, M. Giacca, G. David, S. Fiorentini, A. Caruso, et al., *Blood* 114 (2009) 3335–3342.
- [122] C. He, Y. Hu, L. Yin, C. Tang, C. Yin, *Biomaterials* 31 (2010) 3657–3666.
- [123] V.P. Torchilin, R. Rammohan, V. Weissig, T.S. Levchenko, *Proc. Natl. Acad. Sci. U. S. A.* 98 (2001) 8786–8791.
- [124] V. Estrella, T. Chen, M. Lloyd, J. Wojtkowiak, H.H. Cornell, A. Ibrahim-Hashim, et al., *Cancer Res.* 73 (2013) 1524–1535.
- [125] O. Tredan, C.M. Galmarini, K. Patel, I.F. Tannock, *J. Natl. Cancer Inst.* 99 (2007) 1441–1454.
- [126] K. Kessenbrock, V. Plaks, Z. Werb, *Cell* 141 (2010) 52–67.
- [127] J.S. Rao, *Nat. Rev. Cancer* 3 (2003) 489–501.
- [128] R.K. Jain, T. Stylianopoulos, *Nat. Rev. Clin. Oncol.* 7 (2010) 653–664.
- [129] M.J. Ernsting, M. Murakami, A. Roy, S.D. Li, *J. Controlled Release* 172 (2013) 782–794.
- [130] Z. Gao, L. Zhang, Y. Sun, *J. Control. Release* 162 (2012) 45–55.
- [131] K.N. Sugahara, T. Teesalu, P.P. Karmali, V.R. Kotamraju, L. Agemy, O.M. Girard, et al., *Cancer Cell* 16 (2009) 510–520.
- [132] H. Sha, Z. Zou, K. Xin, X. Bian, X. Cai, W. Lu, et al., *J. Controlled Release* 200 (2015) 188–200.
- [133] H. Sha, R. Li, X. Bian, Q. Liu, C. Xie, X. Xin, et al., *Eur. J. Pharm. Sci.* 77 (2015) 60–72.
- [134] K. Wang, X. Zhang, Y. Liu, C. Liu, B. Jiang, Y. Jiang, *Biomaterials* 35 (2014) 8735–8747.
- [135] W. Song, M. Li, Z. Tang, Q. Li, Y. Yang, H. Liu, et al., *Macromol. Biosci.* 12 (2012) 1514–1523.
- [136] M. Li, Z. Tang, D. Zhang, H. Sun, H. Liu, Y. Zhang, et al., *Biomaterials* 51 (2015) 161–172.
- [137] G. Gu, X. Gao, Q. Hu, T. Kang, Z. Liu, M. Jiang, et al., *Biomaterials* 34 (2013) 5138–5148.
- [138] J. Folkman, *Semin. Oncol.* 29 (2002) 15–18.



Yaqin Zhu is currently a joint PhD candidate between Soochow University and University of Twente under the supervision of Prof. Dr. Zhiyuan Zhong and Prof. Dr. Jan Feijen. She received her B.S. in Medicine from Yangzhou University in 2009 and M.S. in Medicine from Soochow University in 2013. Her current research interests are design and synthesis of smart biodegradable polymers and development of multifunctional nanosystems for tumor-targeted imaging and therapy.



Jan Feijen is a Professor of Polymer Chemistry and Biomaterials at the University of Twente (The Netherlands), Chair Professor at Soochow University Biomedical Polymers Laboratory and Adjunct Professor of Pharmaceutics at the University of Utah. From 1995–2009 he has been the Scientific Director of the Institute for Biomedical Engineering, BMTI, at the University of Twente. His research interests are biomaterials, biodegradable polymers, bio-interfacial phenomena, ring-opening polymerization, hydrogels, drug delivery systems and nano-systems for cancer therapy. He trained 90 PhD students and has co-authored over 600 papers with more than 28.000 citations, H-index 90 (Web of Science). He has served on many editorial boards, was the co-founding editor of the *J. Controlled Release* and has been guest editor for the Journal for many years. Since 1990 he has organized and was the chairman of the first 10 European Symposia on Controlled Drug Delivery Systems, The Netherlands and this series of biannual Symposia is still continuing. Since 2010 he has been the co-organizer of the biannual Symposia on Innovative Polymers for Controlled Delivery (SIPCD) in Suzhou, China. In 2005 he initiated and became a chairman of the Dutch program for Tissue Engineering (DPTE). He is a Fellow of the American Society for Biomaterials, since the start, and a Fellow of the Controlled Release Society. He was former governor of the Controlled Release Society, European Society for Biomaterials and International Society for Artificial Internal Organs. He was a chairman for five years of the Concerted Action on Heart and Replacement Technology, Medical Health Research Programme of the European Community. He has received numerous awards including the Best Paper Award of the *J. Controlled Release*, Controlled Release Society (1992), the Clemson Award, American Society for Biomaterials (1994), the Founders Award, Controlled Release Society, (1998), the George Winter Award, ESB, (2002) and the Award for Distinguished Service in Advancement of Biomaterials Science, Japanese Society for Biomaterials, (2008).



Zhiyuan Zhong is a Distinguished Professor and Chair of Soochow University Biomedical Polymers Laboratory. He received his Ph.D. in 2002 from the University of Twente (The Netherlands). In 2011–2012, he worked as a Vice President of Suzhou BioBay (a top Biomedical Park in China). His research focuses on biomedical polymers, nanomedicine and targeted cancer therapy. He has co-authored about 200 papers with over 12000 times of citation and an H-Index of 61 (Web of Science). He serves as an Associate Editor for *Biomacromolecules* (ACS), a Guest Editor for *J. Controlled Release*, a Promotion Editor for *SCI. CHINA Chem.*, an Editorial/Advisory Board Member for over 10 journals including *Mater. Today*, *J. Controlled Release*, *Nanotechnology*, *Nano Futures*, *J. Gene Med.*, *J. Mater. Chem. B*, *J. Biomater. Sci. Polym. Ed.*, and *Mater. Today Chem.*, and an Executive Chair for the 1st–4th Symposium on Innovative Polymers for Controlled Delivery (SIPCD 2010, 2012, 2014 and 2016) held biennially in Suzhou, China. He has received several prestigious international and national awards including *Biomacromolecules/Macromolecules* Young Investigator Award (ACS), the Friedrich Wilhelm Bessel Research Award (Humboldt Foundation), National Ten-Thousand Talent Award, and National Outstanding Young Scholar Award.